AD-A080 566 SPERRY GYROSCOPE CO GREAT NECK N Y F/G 17/9
COLUMN NETWORK STUDY FOR A PLANAR ARRAY USED WITH AN UNATTENDED--ETC(U)
DEC 79 G L HANLEY, H R PERINI F19628-78-C-0166

UNCLASSIFIED RADC-TR-79-297 NL

1 OF 1
AD
A080566

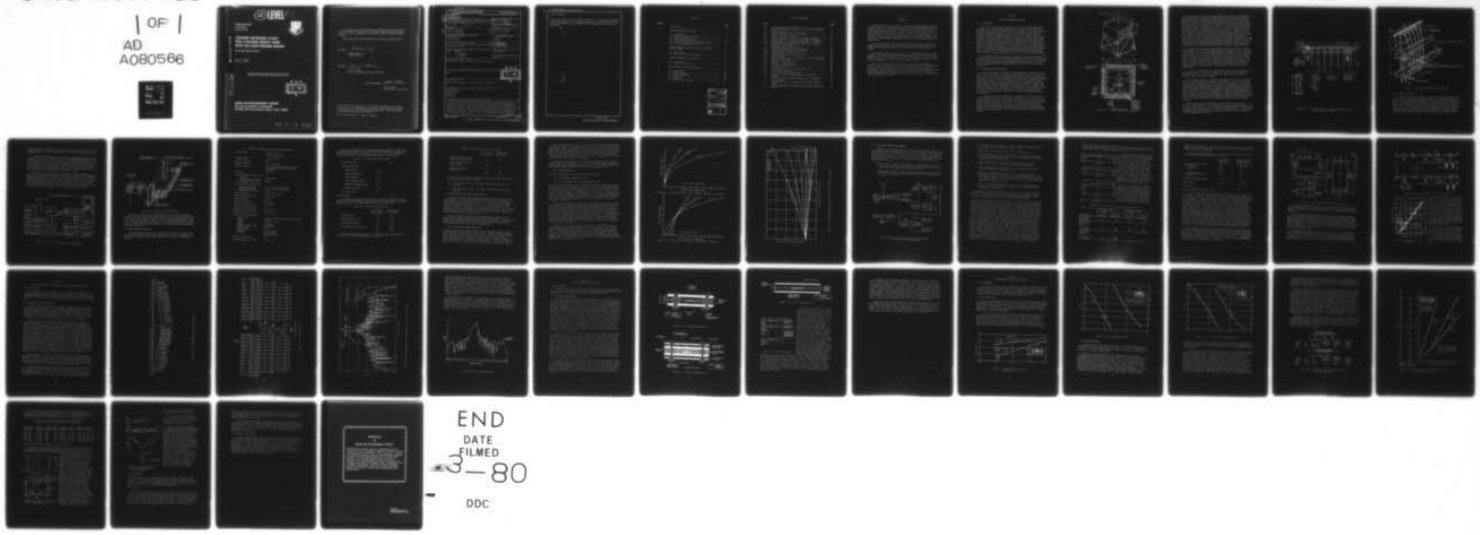

END
DATE FILMED
3-80
DDC

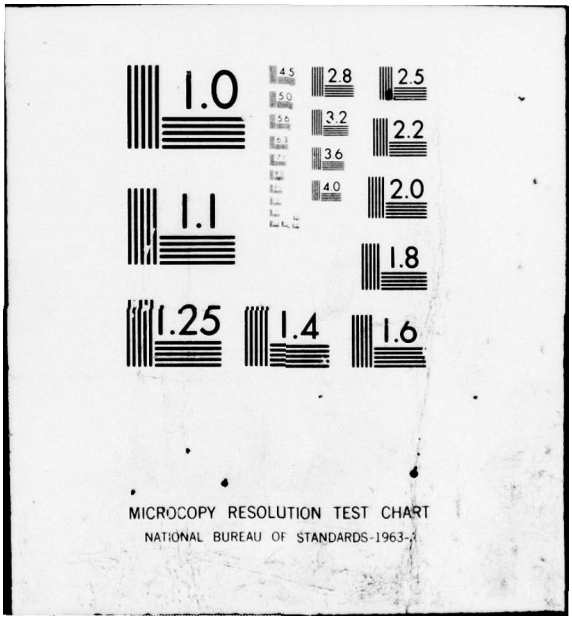
1.0
1.1
1.25
1.4
1.6
1.8
2.0
2.2
2.5
2.8
3.2
3.6
4.0
4.5
5.0
5.6
6.3
7.1
MICROCOPY RESOLUTION TEST CHART
NATIONAL BUREAU OF STANDARDS-1963-A

(12) LEVEL II

RADC-TR-79-297
Interim Report
December 1979

COLUMN NETWORK STUDY FOR A PLANAR ARRAY USED WITH AN UNATTENDED RADAR

Sperry Gyroscope Company

Gerald L. Hanley
Harry R. Perini

APPROVED FOR PUBLIC RELEASE; DISTRIBUTION UNLIMITED

ROME AIR DEVELOPMENT CENTER
Air Force Systems Command
Griffiss Air Force Base, New York 13441

This report has been reviewed by the RADC Public Affairs Office (PA) and is releasable to the National Technical Information Service (NTIS). At NTIS it will be releasable to the general public, including foreign nations.

RADC-TR-79-297 has been reviewed and is approved for publication.

APPROVED: Gregory Cruz

GREGORY CRUZ, 1 Lt
Project Engineer

APPROVED: Allan C. Schell

ALLAN C. SCHELL
Chief, Electromagnetic Sciences Division

FOR THE COMMANDER: John P. Huss

JOHN P. HUSS
Acting Chief, Plans Office

If your address has changed or if you wish to be removed from the RADC mailing list, or if the addressee is no longer employed by your organization, please notify RADC (EEA) Hanscom AFB MA 01731. This will assist us in maintaining a current mailing list.

Do not return this copy. Retain or destroy.

UNCLASSIFIED

SECURITY CLASSIFICATION OF THIS PAGE (When Data Entered)

REPORT DOCUMENTATION PAGE	READ INSTRUCTIONS BEFORE COMPLETING FORM
1. REPORT NUMBER: RADC-TR-79-297	2. GOVT ACCESSION NO. / 3. RECIPIENT'S CATALOG NUMBER
4. TITLE (and Subtitle): COLUMN NETWORK STUDY FOR A PLANAR ARRAY USED WITH AN UNATTENDED RADAR	5. TYPE OF REPORT & PERIOD COVERED: Interim Report 6. PERFORMING ORG. REPORT NUMBER: N/A
7. AUTHOR(s): Gerald L. Hanley, Harry R. Perini	8. CONTRACT OR GRANT NUMBER(s): F19628-78-C-0166
9. PERFORMING ORGANIZATION NAME AND ADDRESS: Sperry Gyroscope Co., Great Neck, L. I. NY 11020	10. PROGRAM ELEMENT, PROJECT, TASK AREA & WORK UNIT NUMBERS: 12412F, 46001402
11. CONTROLLING OFFICE NAME AND ADDRESS: Deputy for Electronic Technology (RADC/EEA), Hanscom AFB MA 01731	12. REPORT DATE: December 1979 13. NUMBER OF PAGES: 44
14. MONITORING AGENCY NAME & ADDRESS (if different from Controlling Office): Same	15. SECURITY CLASS. (of this report): UNCLASSIFIED 15a. DECLASSIFICATION/DOWNGRADING SCHEDULE: N/A

16. DISTRIBUTION STATEMENT (of this Report)

Approved for public release; distribution unlimited.

17. DISTRIBUTION STATEMENT (of the abstract entered in Block 20, if different from Report)

Same

DDC RECEIVED FEB 7 1980 B

18. SUPPLEMENTARY NOTES

RADC Project Engineer: Gregory Cruz, 1 Lt (RADC/EEA)

19. KEY WORDS (Continue on reverse side if necessary and identify by block number)

Column Network
Planar Array
Stripline
Dual Beam

20. ABSTRACT (Continue on reverse side if necessary and identify by block number)

Objectives of this program are to investigate design and fabrication techniques for an azimuthally phase-steerable planar array with dual-beams for elevation coverage. Network costs, network insertion loss, antenna pattern performance, and reliability are significant considerations. A stripline dual beam column network is being designed, fabricated and tested to demonstrate achievable performance and competitive techniques for production and installation costs are being studied. This report summarizes the work completed (Cont'd)

DD FORM 1 JAN 73 1473

UNCLASSIFIED

230 800 SECURITY CLASSIFICATION OF THIS PAGE (When Data Entered)

Item 20 (Cont'd)

during the first half of the program: completion of the Antenna Conceptional design, development of all the required components, the design of the dual beam column network, and preliminary results of competitive techniques for production.

CONTENTS

LIST OF ILLUSTRATIONS

Section 1

INTRODUCTION

The objectives of this program are to investigate design and fabrication techniques for an azimuthally phase-steerable planar array with dual beams for elevation coverage. The potential application is for unattended strategic ground radar systems which will be located in remote arctic areas. The unattended radars are intended to be a means of reducing operating costs associated with the present DEW Line system, as well as to improve present surveillance coverage against low flying targets. Network costs, network insertion loss, antenna pattern performance, and reliability are significant considerations.

During this program, a stripline dual beam column network is being designed, fabricated, and tested to demonstrate achievable performance. Also, competitive techniques for production and installation costs are being studied.

The progress during the first half of the program has resulted in completion of the Antenna Conceptual Design, the development of all the required components, and the design of the dual beam column network. The study of competitive techniques for production have been started, and preliminary results show the feasibility of a low cost, light weight design.

Section 2 describes the progress in the general array configuration studies. Section 3 describes the status of the dual beam column network which is being built, and which will be tested to demonstrate antenna pattern performance. Section 4 describes the various stripline fabrication techniques being considered with emphasis on ease of fabrication and cost reduction. Section 5 describes the development of the stripline components which are used in the column network layout.

Section 2

ANTENNA CONFIGURATION STUDIES

2.1 TASK SUMMARY

This section describes an investigation of the design and fabrication techniques for a 2-D, azimuthally steerable, four-faced planar array for application to unattended, ground-based, search radars. The design approach utilizes a square configuration of four planar phased arrays to provide 360-degree azimuthal surveillance coverage to fifteen thousand feet in altitude, with an instrumented range of sixty nautical miles. The elevation coverage is achieved using two contiguous beams which provide coarse target elevation data and facilitate the use of optimized signal processing techniques for low and high elevation targets independently. To achieve this elevation coverage, the four planar arrays contain vertical column networks comprising radiator elements and low loss microwave power distribution networks. The network is capable of simultaneously generating the illumination function for the low and high beams, respectively, through discrete input ports. An objective of this task effort is to identify the requirements imposed upon the column network by selection of the baseline antenna design.

The workscope associated with this task involves (1) examination of the baseline antenna design, (2) antenna performance evaluation, (3) definition of physical parameters, component packaging, and assembly concept, (4) evaluation of structural requirements and environmental impact factors, and (5) conceptual design selection. The study results are described in the following subsections.

2.2 BASELINE ANTENNA DESCRIPTION

A baseline antenna configuration has been generated consisting of four planar array faces mounted in a square configuration on top of a tower platform. Each array provides coverage against airborne targets at elevations from ground level to fifteen thousand feet and within an instrumented range of sixty nautical miles. Dual fixed beam elevation coverage permits separate, independent, signal processing techniques for the two elevation regimes. Phase steerable azimuth scan capability provides $\pm$ 45-degree coverage from each array face, thereby enabling a full 360-degree azimuth coverage. The antenna is designed for installation and operation in a severe arctic environment as part of an unattended radar system. As such, its components are designed for low loss, high reliability, low power consumption, and easy maintainability.

The baseline antenna configuration, figure 2-1, consists of four 12 by 24-foot planar arrays mounted in a square configuration on a tower with a maximum height of 100 feet. Each array face consists of 59 vertical column network boards spaced 4.9 inches apart. The tower structure will have its legs sunk into an excavation deep enough to stand on perpetually frozen ground. The array and mounting structure are designed to withstand the extremes of arctic operation, including wind velocities of 100 mph, ambient temperatures varying between -35 and +100 degrees Fahrenheit, and peak snow loading.

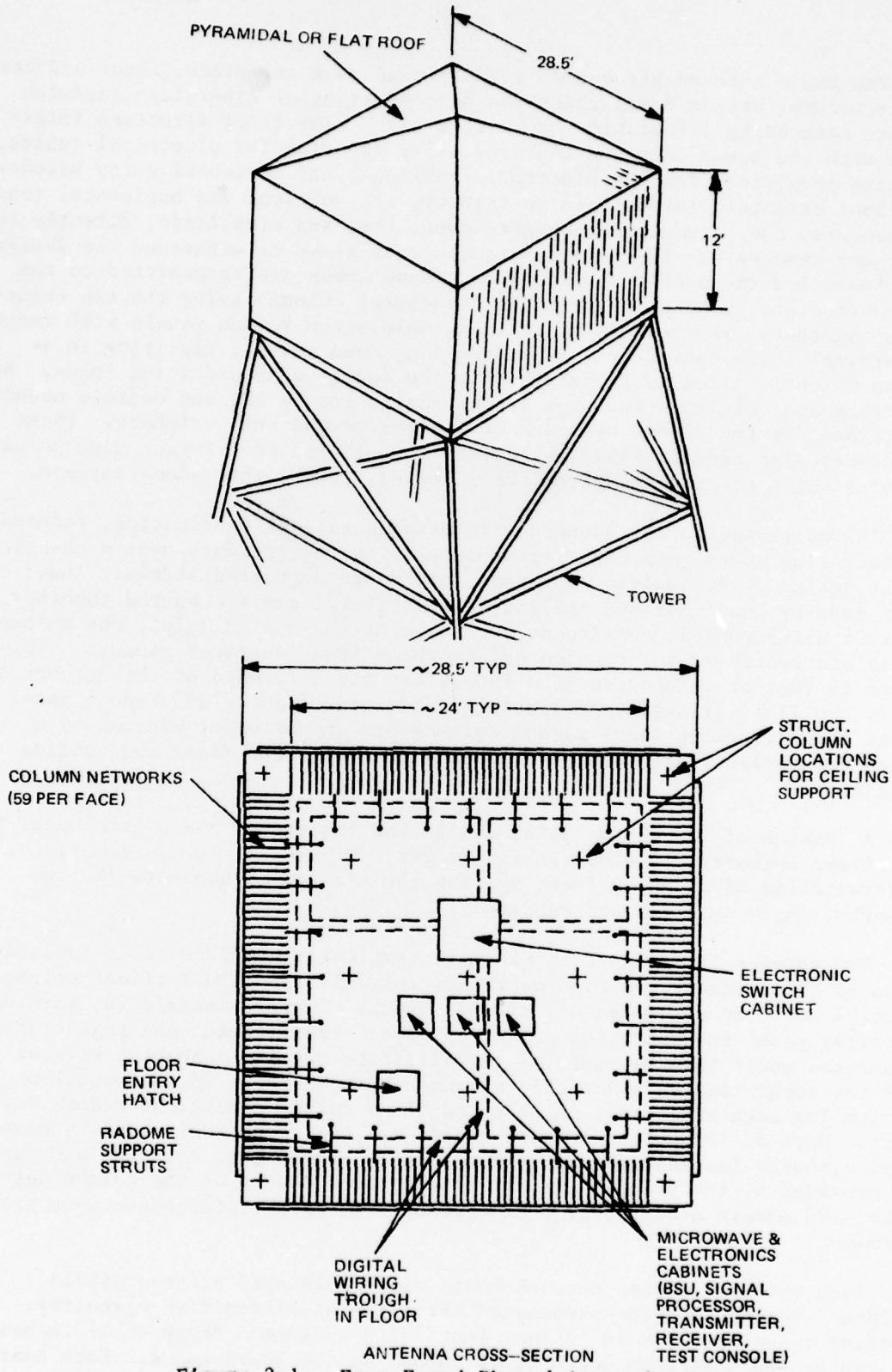

Figure 2-1. Four-Faced Phased Array Antenna

The basic antenna structure is envisioned as a one-piece, floor and ceiling structure, with a modularized radome consisting of fiberglass sandwich panels, each being 5 feet wide by 12 feet high. The floor structure interfaces with the tower deck and contains false flooring for electrical cables, mounting provisions for the electronic cabinets, and personnel entry hatches. The floor structure is designed to transmit all vertical and horizontal loads and moments, due to equipment weight, snow, ice, and wind loads, directly to the tower structure. The ceiling structure is sized to withstand the design snow loads for the arctic application. These loads are transmitted to the floor structure by means of vertical structural columns tying the two structures together. The columns effectively unload the radome panels with respect to vertical loads caused by snow and ceiling dead weight, resulting in a radome which is sized to withstand only the design wind and icing loads. Both the floor and ceiling structures are thermally insulated, and contain mounting provisions for the radome by means of flanges around the periphery. These structures also contain slide mechanisms to position the 12-foot high column networks which are inserted from the interior, toward the radome surface.

The multi-sectioned radome design affords ease of fabrication, reduced manufacturing costs, and eased transportability requirements over a one-piece planar design. The individual radome panels are supported at their lower and upper ends by the floor and ceiling, respectively, and are butted together to create a site-erected, continuous surface. At the butted joint, the radome panels are bolted to a T-section column which lends vertical support. This column is further reinforced by a fiberglass block forward of the network dipoles. To limit allowable deflections under wind loading and radome panel stress levels, the vertical radome columns are supported at midspan by a pinned triangular frame structure, tied directly to the floor and ceiling structures.

A sketch of the radome joint design and the ground plane attachment for the column networks, is shown in figure 2-2. Figure 2-3 is a schematic representation of an array face, showing the radome, column network, row networks, phase shifters and cabling.

The antenna is designed to minimize complexity and on-site installation, while still maintaining a high degree of reliability. The vertical column networks would be assembled off-site in groups of approximately 10, forming six array panel subassemblies per array face. Prealignment and registration techniques would then be employed to facilitate on-site assembly, without the need for sophisticated and costly alignment procedures. Environmental protection for each array face is provided via a coated fiberglass radome cover sheet. Each of the column network boards are sealed at their ends by means of metal closures fastened to the ground planes. Structural rigidity and support are provided by the printed circuit board ground planes of the column networks. To obtain a high degree of reliability, cable interconnections are minimized.

Each vertical column network board will contain 25 printed dipole radiator elements and the associated stripline elevation feed circuitry. The baseline column network is 12 feet long, with a maximum depth of 27 inches at the center and a minimum depth of 15 inches at the board edges. Each board is estimated to weigh approximately 13 pounds, resulting in a total weight of about 800 pounds per array face.

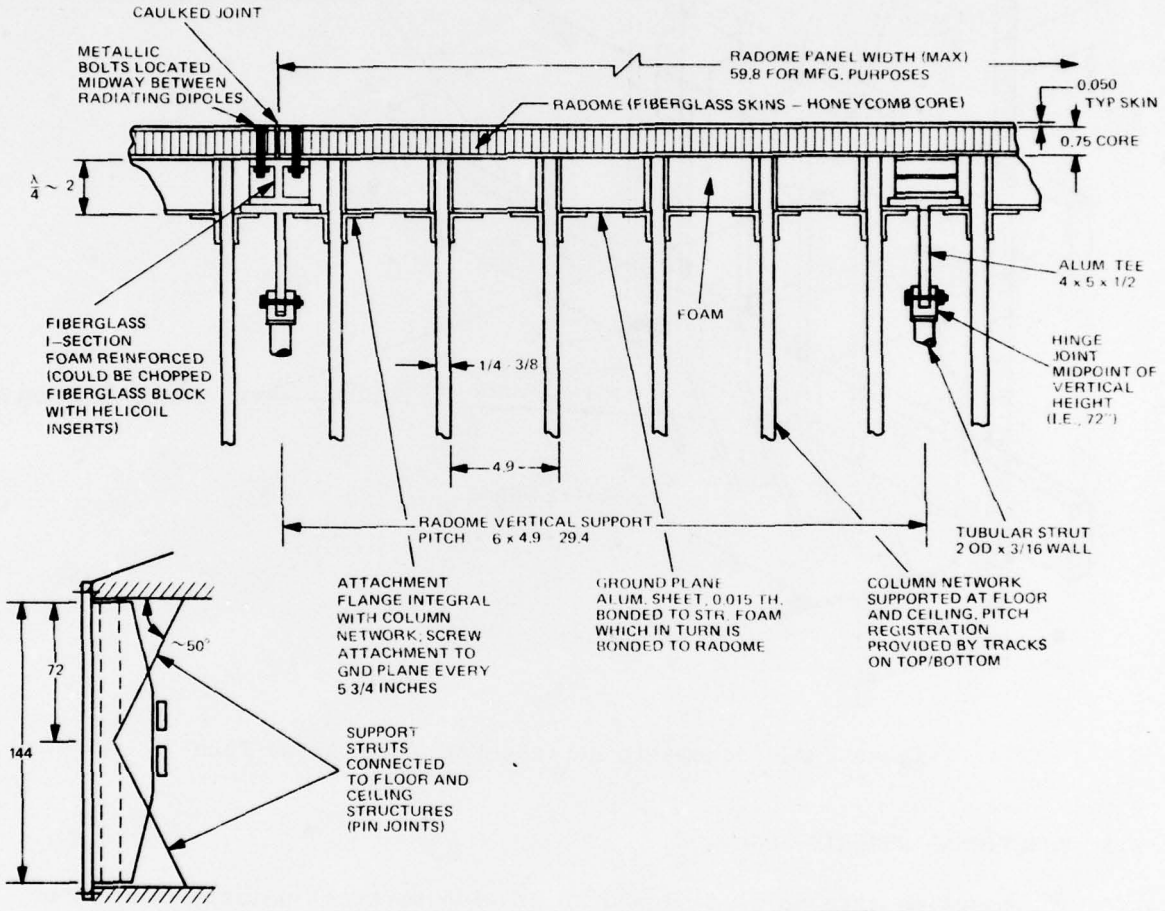

Figure 2-2. Structural Details of Ground Plane Connection and Radome Support Structures

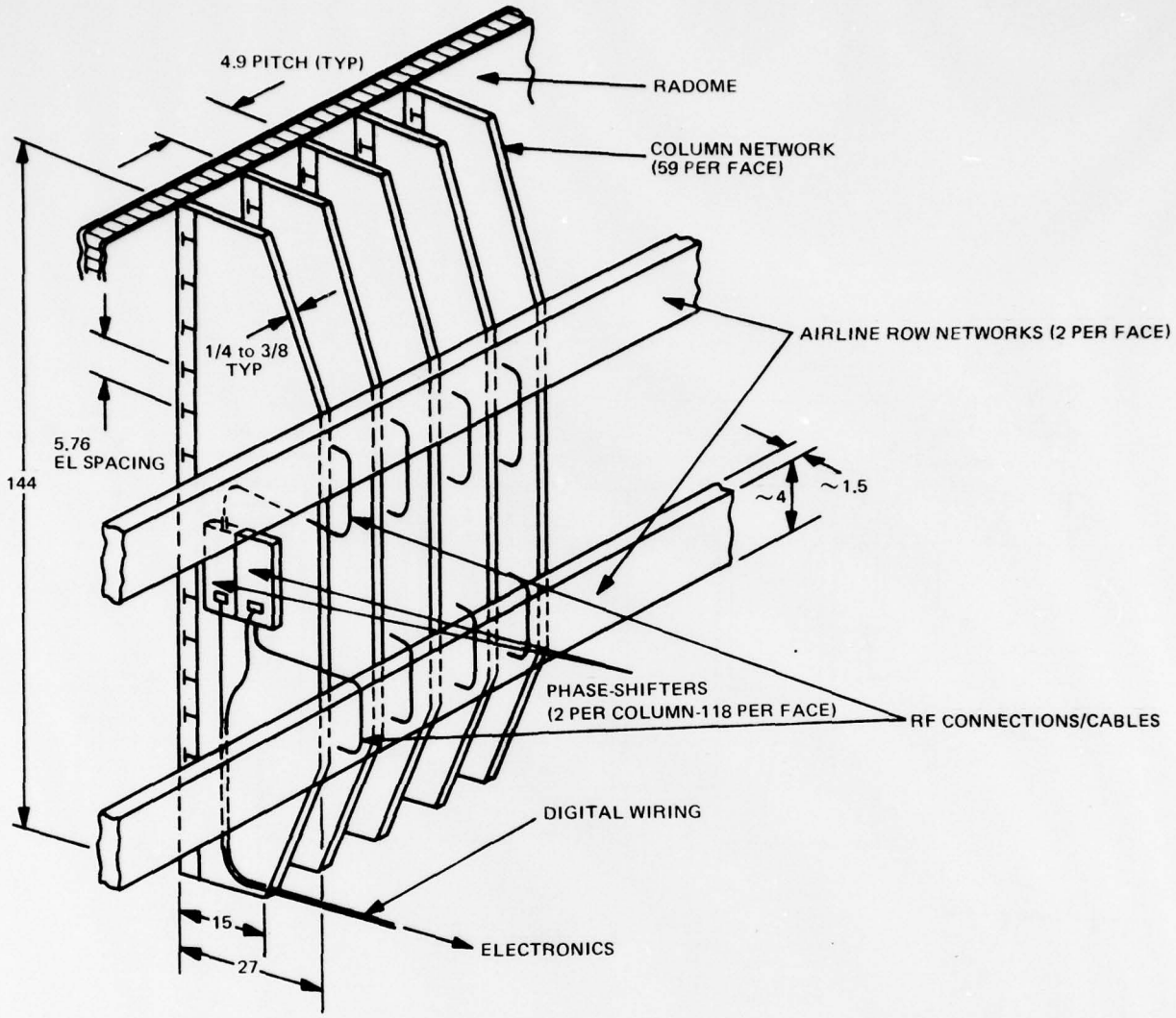

Figure 2-3. Schematic Representation of Array Face

2.3 FUNCTIONAL DESCRIPTION

The baseline antenna is designed to provide vertical polarization with constant gain coverage against airborne targets at elevations from ground level to five degrees above the horizon, and constant elevation coverage from five to thirty degrees above the horizon. To accomplish this, the antenna provides two simultaneous elevation beams generated via center-fed, dual-channel vertical column networks. The lower beam provides the constant gain coverage from 0 to 5 degrees; the upper beam provides a cosecant squared (constant elevation) coverage from 5 to 30 degrees. The antenna is phase steerable $\pm$ 45 degrees in azimuth via two separate sets of phase shifters.

Thus, simultaneous and independent control for each beam is realized, thereby enabling optimized processing algorithms to be utilized in each of the two channels.

A functional block diagram of the baseline antenna showing the key components, is presented in figures 2-4 and 2-5. Because of the quantities required, the vertical column network is a major key component. This is a low loss, single layer stripline, center-fed tandem series network which generates two independent array excitations corresponding to the two elevation beams. The stripline distribution network, designed to have less than 1.0 dB loss over the operating band, excites a set of printed stripline dipoles which are the vertically polarized radiating elements of the array.

The antenna is sized to provide a 2.0-degree azimuth beamwidth at the horizon. The elements are spaced for $\pm$ 45-degree azimuth scan for both beams, without any deleterious effect due to grating lobe conditions. Azimuth scan capability is provided via two sets of digital diode phase shifters. Diode phase shifters are used for the baseline antenna because of their inherent cost and packaging advantages at these frequencies. The required number of phase shifter bits is a function of the desired sidelobe performance. For the 25-dB baseline sidelobe design, 5-bit phase shifters are selected.

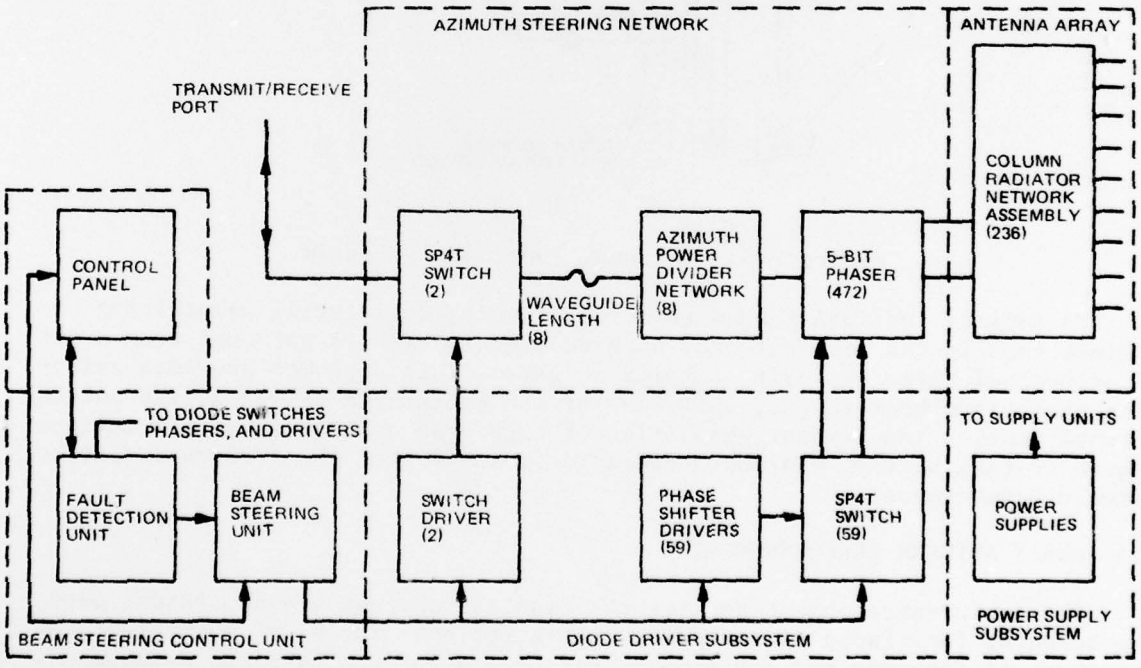

Figure 2-4. Four-Faced Planar Array, Block Diagram

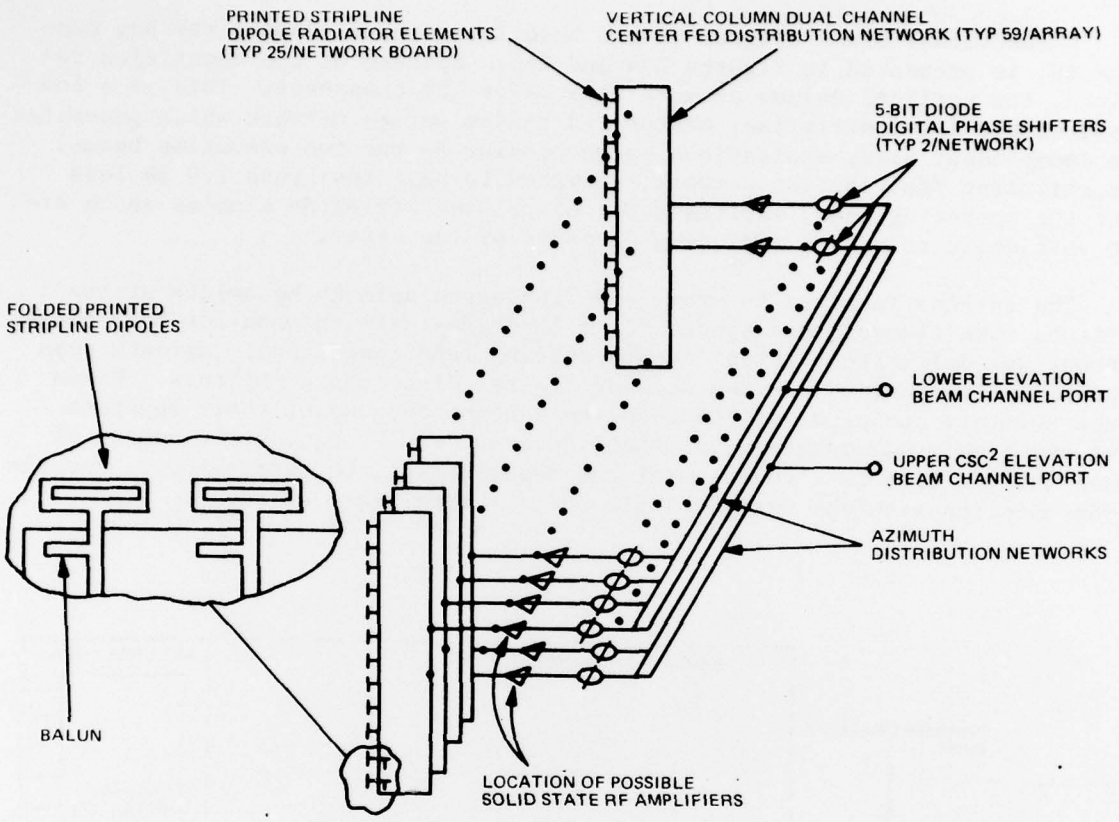

Figure 2-5. Antenna, Functional Diagram

To satisfy the dual shaped beam requirments, while still maintaining minimum loss in the feed network, each beam excitation is selected from a set of orthogonal beams employing complex weights. This approach provides selection of optimum beam shapes, while use of the center-fed tandem series column network enables independent generation of each beam excitation with a maximum degree of flexibility, minimum network loss, and better than -20 dB isolation between beam channels.

2.4 ARRAY ANTENNA PERFORMANCE

The performance objectives for the baseline antenna are consistent with the selected four-faced planar array configuration. Table 2-1 summarizes the key physical features and performance parameters for the baseline antenna concept.

Table 2-1. Baseline Antenna Summary Description

Antenna Type	Square four-faced Planar phased array
Frequency Band	1.2 to 1.4 GHz
Azimuth Coverage	360°
Elevation Coverage	0 to 15,000 feet
Design Features	Low loss, high reliability and easy maintainability for severe arctic environment
Peak Gain	30.5 dB
Azimuth Pattern of Planar Array	
Beamwidth	2° broadside
Electronic Beam Steering	±45°
Maximum Sidelobe Level	-25 dB
Elevation Pattern (Dual Beam)	
Lower Beam Coverage	0 to 5° (nominally uniform)
Upper Beam Coverage	5 to 30° cosecant squared
Maximum Sidelobe Level	-15 dB
Phase Shifter Type	5-bit digital diode
Number of Phase Shifters	118 per face
Antenna Height	12 feet
Planar Array Width	24.1 feet
Column Network Spacing	4.9 inches
Number of Column Networks	59
Radiator Element Spacing	5.76 inches
Number of Radiator Elements	25 per column
Column Network Description	
Network Type	Center-fed tandem, stripline series feed
Height	12 feet
Depth	15 to 27 inches
Weight	13 pounds
Radiator Element Type	Folded dipole
Polarization	Vertical
Maximum VSWR	1.3
Isolation	-20 dB minimum
RF Power	500 watts peak 20 watts average
Maximum Insertion Loss	1 dB
Operating Temperature Range	-35 to 100°F

The gain and losses for the baseline antenna are itemized in table 2-2. The directivity is based upon a broadside azimuth beamwidth of 2 degrees and an elevation beamwidth of 5 degrees for the low beam. Antenna component losses are based upon expected hardware performance characteristics.

Table 2-2. Antenna Gain and Loss Budget

Directivity (dB)		35.0
Antenna Losses (dB)		
Column Network	1.0	
Diode Phase Shifters	1.2	
Azimuth Network	0.7	
Interconnecting Cables	0.3	
Quadrant Transmission Line	0.3	
Commutation Switch	1.0	
Total Losses (dB)	4.5	
Power Gain (dB)		30.5

Array phase and amplitude tolerances of 6.8 degrees rms and 0.25 dB rms, respectively, are the maximum allowable for peak azimuth sidelobes of -25 dB. The array tolerances are allocated as shown below in table 2-3.

Table 2-3. Array Tolerance Allocation

	rms Phase Error (degrees)	rms Amplitude Error (dB)
Azimuth Network	3.0	0.15
Digital Phase Shifters	5.0	0.15
Interconnecting Cables	2.5	0.10
Error Between Column Networks	2.5	0.10
	6.8	0.25

The column network phase error of 2.5 degrees rms and amplitude error of 0.1 dB rms are allocated as shown below in table 2-4.

Table 2-4. Column Network Error Allocation

	rms Phase Error (degrees)	rms Amplitude Error (dB)
Amplitude and Phase Error Between Column Networks	1.78	0.1
Transverse Position Error (±0.125 inch)	1.01	-
Axial Position Error (±0.125 inch)	1.43	-
	2.5	0.1

For -15 dB peak elevation sidelobes, the tolerance error budget within a column network is specified as follows:

a) for correlated errors: 8.2 degrees rms phase and 0.2 dB rms amplitude

b) for uncorrelated errors: 15.6 degrees rms phase and 0.4 dB rms amplitude.

2.5 BEAM POINTING ERROR FOR THE PLANAR ARRAY

An azimuth pointing error results when scanning a planar array fan beam from broadside. For the lower 5-degree beam of the baseline antenna, the azimuth error is less than 0.2° over the ±45° scan sector. For the upper fan beam, with the error normalized to zero at 15° in elevation, the maximum azimuth pointing error is typically -1.7° at 5° elevation and 3.9° at 25° elevation for ±45° of azimuth scan. The azimuth angle estimation error can be reduced by comparison of estimates from adjacent array faces. This, however, would increase the baseline array cost by requiring additional hardware to provide increased azimuth scan capability.

Because of beam characteristics, an azimuth angle estimation error results when scanning a planar array fan beam from broadside. This error is inherent to the scanning characteristics of the planar array, increasing with azimuth angle from the array normal and for increasing fan beam elevation angle. The azimuth angle error can be expressed as:

$$\alpha = \sin^{-1} [\sin \alpha_0 \cos \beta_0 / \cos \beta] - \alpha_0$$

where α_0 is the selected azimuth angle, β is the elevation angle, and β_0 is the assigned elevation angle for zero error. Figure 2-6 shows the azimuth angle error as a function of elevation angle for azimuth scan angles of α_0 = 30, 45, and 60 degrees, with $\beta_0 = 0°$. At an elevation angle of 20 degrees, for example, the azimuth error would be 2.1, 3.8, and 7.1 degrees for azimuth scan of 30, 45, and 60 degrees, respectively. These results would be typical for a single fan beam case and with independent planar array faces.

The azimuth angle error would be reduced for the baseline dual elevation beam system. Since the lower beam is only used over a 5° elevation range, the azimuth error would be less than 0.2° over the ±45° scan sector. The azimuth angle error is also reduced for the upper beam by adjusting for zero error at a selected elevation angle. Figure 2-7 shows the azimuth angle error normalized to zero at β_o = 15 degrees. For this case, at 30, 45, and 60 degrees of azimuth scan, the error is, respectively, -1.0, -1.7 and -2.9° at 5° elevation, and 2.2, 3.9 and 7.4° at 25° elevation.

Over limited scan regions, for the four-faced planar array, the target azimuth and elevation angles can be estimated by comparing beam information from adjacent faces to minimize the angle pointing error. For the upper beam, the resulting azimuth angle estimation error can be expressed as:

$$\alpha_{12} = (C\,\alpha_1 + \alpha_2)/(C + 1)$$

where C is a weighting coefficient dependent upon α_o and

$$\alpha_1 = \sin^{-1}\,[\sin\alpha_o \cos\,\beta_o/\cos\beta\,] - \alpha_o$$

$$\alpha_2 = \sin^{-1}\,[\sin(\,\alpha_o - 90°)\cos\,\beta_o/\cos\beta\,] - [\alpha_o - 90°]$$

By increasing the azimuth scan angle to ±60 degrees, for example, the azimuth pointing error could be reduced in the overlap region for scan angles greater than ±30 degrees. For the baseline upper beam case, the maximum error would then be described by the α_o = 30-degree curve on figure 2-7. This results in a worst case maximum error of 3.9 degrees for a target at a 30-degree elevation. Figure 2-8 shows the azimuthal error versus scan angle from broadside for various target elevation angles. This 45-degree azimuth sector provides planar array error characteristics which would be typical for the entire 360-degree scan region.

The error characteristics which have been generated represent a preliminary estimate for a four-faced planar array. Additional contributors to the beam pointing error include antenna and receiver instrumentation accuracy, clutter and multipath effects, and thermal noise limitations. The pointing error due to thermal noise on a constant amplitude target, for example, is proportional to the beamwidth and is inversely proportional to the square root of the number of samples and to the signal-to-noise level. In the cross-over region between planar array faces, the beamwidth increases and the antenna gain decreases approximately proportionally to the cosine of the scan angle, which would generally require an increased number of samples to maintain the pointing accuracy capability.

Examination of the azimuth beam pointing error for the baseline four-faced planar array indicates that the error may be reduced in the overlap region by reducing the column network spacing to provide increased azimuth scan. If, for example, each array face were designed for ±60-degree azimuth scan, then the maximum element spacing reduces to 4.435 inches. This corresponds to a 9.1 percent increase in the number of column networks for a given aperture width. A more detailed systems analysis is required to determine the allowable antenna pointing accuracy.

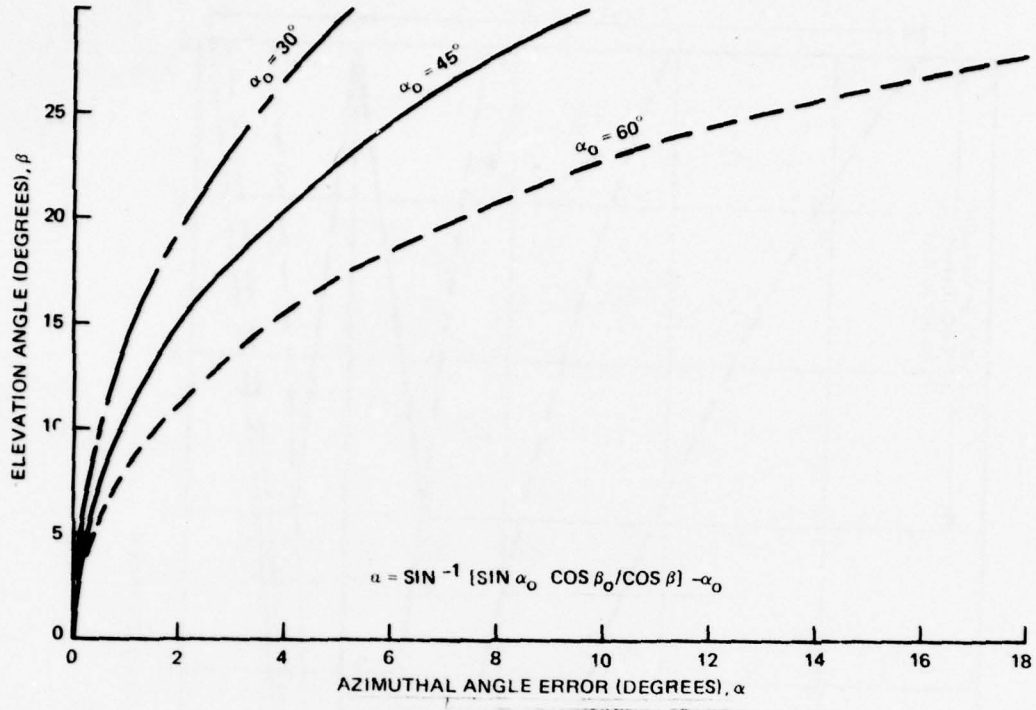

Figure 2-6. Azimuth Angle Error Versus Elevation Angle (β_o = 0 Degrees)

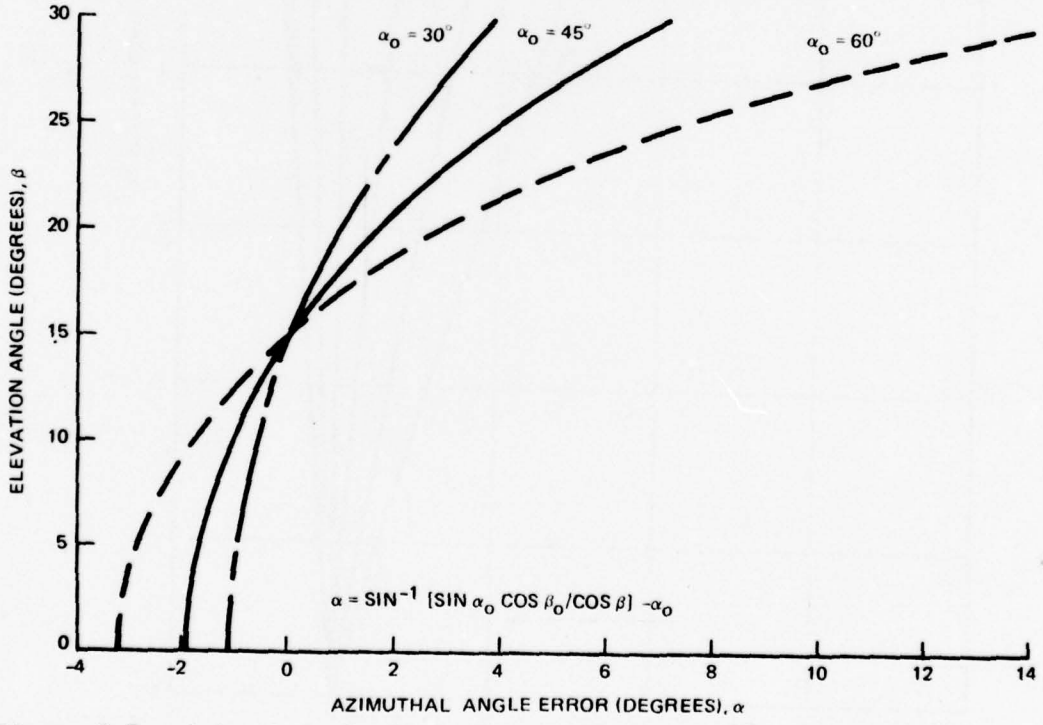

Figure 2-7. Azimuth Angle Error Versus Elevation (β_o = 15 Degrees)

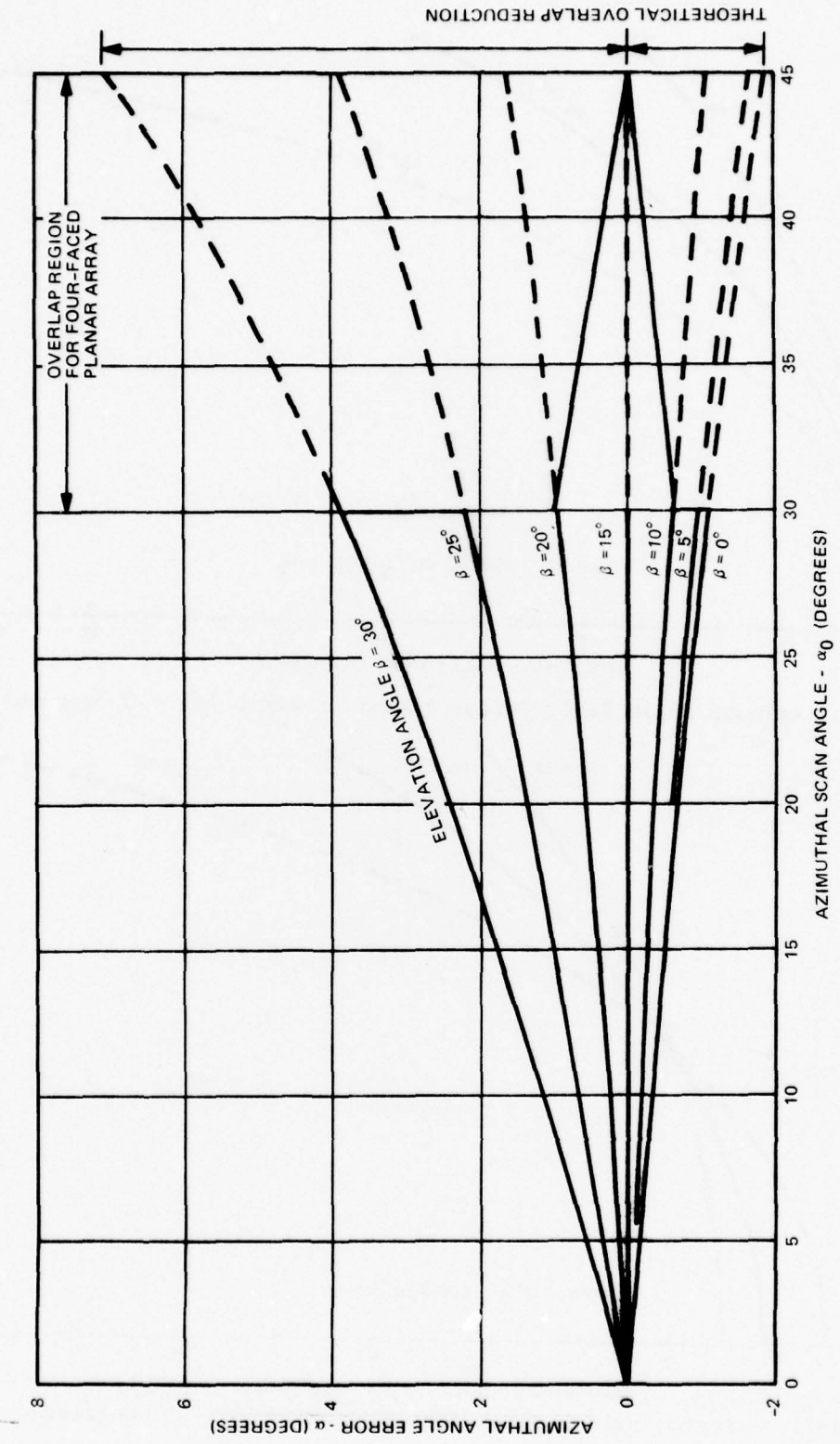

Figure 2-8. Azimuth Angle Error Versus Scan Angle (β_o = 15 Degrees)

2.6 SOLID STATE TRANSMITTER TRADE-OFF

A number of RF configurations were evaluated in detail for a solid state transmitter system. The major objective was to select a cost effective system that would provide low power consumption and high reliability. The candidate configurations consisted of locating the major power amplifiers at three different extreme locations in an antenna system with 59 column networks for each planar array face. As indicated in figure 2-9, these candidate positions included the following:

- Solid State Big Bottle - The required transmit RF power is obtained from a big bottle solid state amplifier assembly located at the input to an azimuth and elevation RF distribution system.

- Intermediate Amplifier Modules - Separate amplifier modules located at each output of an azimuth distribution network prior to SP4T sector switches. (Qty - 59).

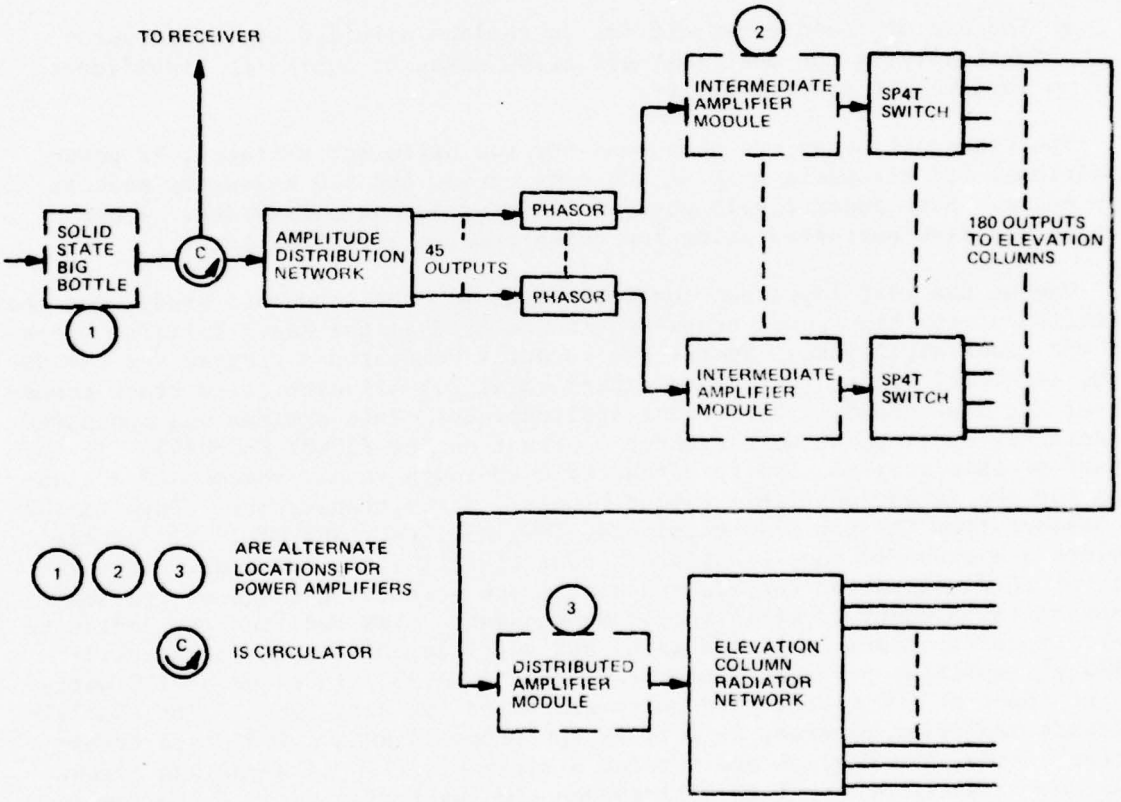

Figure 2-9. RF System with Three Alternative Locations for Power Amplifiers, Block Diagram

- Distributed Amplifier Modules - Separate amplifier modules located at the input to each column network. (Qty - 236).

The important conclusions from the trade-off investigations are:

- When the RF amplifiers are located closer to the radiating elements, the system becomes more efficient, since the amplifiers do not have to overcome the RF distribution losses.

- Amplification at the elements in a commutating planar array is more costly, since it requires more transistors and modules.

- The optimum approach will generally be a compromise between prime power consumption and implementation cost.

- A typical configuration is described using intermediate module amplifiers, located at each output of an azimuth network, for the low beam transmit signal, and a medium power solid state bottle to provide the transmit signals for the upper beam and the drive signals for the intermediate amplifiers module.

- The use of stand-by-amplifiers to replace a failed amplifier automatically is the most cost-effective means of achieving significant improvement in reliability.

The trade-off study was performed for two different radiated, RF power conditions; 2.5 kilowatts peak at 10% duty cycle, and 5.0 kilowatts peak at 7% duty cycle. Both power levels were at 100-microsecond pulsewidth. A comparison was also performed using low noise receive amplification.

One of the most important considerations for the trade-off study, was the selection of the high power transistor to be used as the basic building block for the power amplifiers. Sperry has recently completed a program for the design, fabrication, and test of an experimental 2.5-kilowatt solid state transmitter for unattended, L-band radar applications. This program was sponsored by Rome Air Development Center under contract number F30602-F-C-0245. At the outset of this program, Sperry conducted a thorough vendor search and evaluation for the latest available L-band bipolar, power transistors. This included devices from the top four suppliers, TRW, MSC, PHI, and CTC. All of the devices are grounded base transistors operating in a class C mode. As a result of this evaluation the TRW transistor was selected because of its substantial improvement in efficiency. Subsequently, TRW modified the device to Sperry specifications (improved gain) and supplied 80 devices for the 2.5-kilowatt amplifier program. This transistor (MRA-296) is rated at 100 watts output power at 100 microsecond pulse width and 10% duty cycle. For the 2.5-kilowatt amplifier program, as well as the proposed RRAS solid state transmitter system, the devices are derated a minimum of 15% to a maximum output power of 85 watts peak. This will reduce the power dissipated in the device and lower junction temperatures to conservative levels, thereby achieving high reliability operation. Reducing the transistor output power requires the use of more devices to obtain the required transmit levels. Consequentyly, the derating factor is a compromise between cost and reliability. The typical

performance for the MRA-296 transistor is presented in figure 2-10. As indicated, the minimum performance over the 1215 to 1400 MHz frequency range is 85 watts output power, 7.5 dB gain, and 52% efficiency.

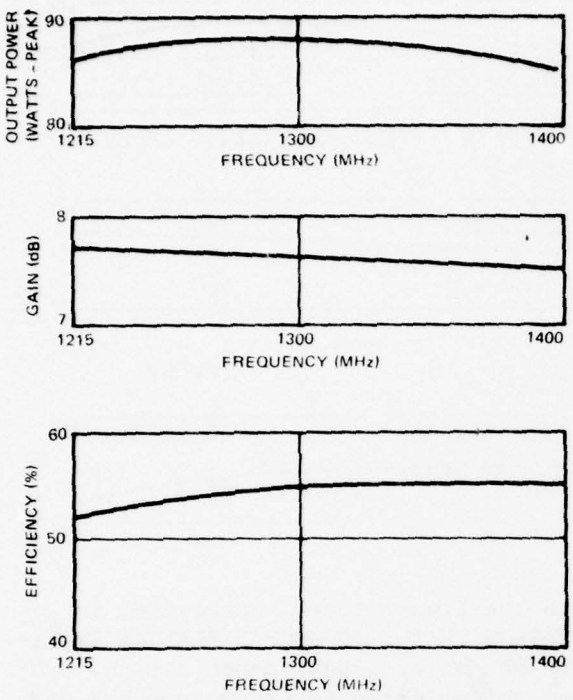

Figure 2-10. TRW MRA-296 Transistor Test Data

With the MRA-296 transistor as the basic building block, a trade-off study was performed for the three transmitter configurations previously described. The results of this investigation are summarized in comparison in table 2-4. As the RF amplifiers are located closer to the radiating elements, the transmitter system becomes more efficient and the prime power is reduced. However, amplification at the elements in a commutating planar array is more costly since it required more transistors and modules. Consequently, the optimum approach will be a compromise between prime power consumption and costs.

As a result of the above trade-off investigation, a typical solid state transmitter configuration might utilize a combination of a medium power bottle (solid state transmitter) and intermediate transmit amplifier modules with a total radiated power of 2.5 kilowatts. The solid state transmitter would provide the transmitter power for the upper beam and the drive signals for the

Table 2-4. Solid State Transmitter Comparison Results

	2.5-kilowat Transmit Power		5.0-kilowat Transmit Power	
Configuration	Relative Cost System	Prime Power (watts/sys)	Relative Cost System	Prime Power (watts/sys)
SOLID STATE BIG BOTTLE	1.0	860	1.7	1200
INTERMEDIATE MODULE				
• W-LNA	1.9	370	3.0	550
• W/O-LNA	1.6	600	2.5	740
DISTRIBUTED MODULE				
• W-LNA	4.0	250	-	-
• W/O-LNA	3.6	430	-	-

transmit amplifier modules. The final amplification for the low beam transmit signal is provided by the transmit amplifier modules located in each output of an azimuth distribution network.

The anticipated performance and parameters for the solid state transmitter and transmit amplifier modules are as follows:

	Solid State Transmitter	Transmit Amplifier Modules (45)
Output Power (watts, peak)	450	2330 (total)*
Gain (dB)	26.5	17
Efficiency	37%	42%
Vcc	28v/32v	28v
Prime Power (watts, avg) (10% DC)	120	560
MTTR (replace spare module)	1/2 hr	1/2 hr
Size (inches)	12 x 8 x 6	60 x 12 x 6
Weight (lbs)	10	80

*Includes amplitude tapering effect.

A block diagram for a typical solid state transmitter is presented in figure 2-11. It consists of a driver module with two identical 3-stage amplifier channels connected at their input and output by a SPDT diode switch. One of the channels is a standby unit that is automatically switched into the circuit when there is a failure to the operating channel. The output from the driver module is distributed equally to 6 of the 7 paralleled output stage transistors, through a 1P6T power divider/switch network. The 7th output transistor amplifier is a standby unit that is automatically switched into the circuit when there is a failure to any of the 6 operating amplifiers. The output power from the 6 operating transistors is efficiently combined in an identical 1P6T power combiner/switch network. These networks are stripline, center fed, reactive, power dividers with shunt mounted diodes in each of the 7 output arms located a quarter wavelength from the center junction. The input signal can be distributed equally to any 6 of the 7 output with the proper biasing of the diodes. With 1-watt peak RF input power, the solid state transmitter will provide 450 watts peak output power at a collector voltage of 31 volts. About 370 watts will be used for the upper beam and the remainder (80 watts) to drive the 59 transmit amplifier modules for the low beam.

This concept of self-healing, using stand-by amplifiers that automatically replace failed units, has been demonstrated by Sperry during the acceptance tests of the 2.5-kilowatt solid state, L-band transmitter developed for RADC. Reliability calculations for the RADC program indicated 2 orders of magnitude improvement in reliability with the use of one standby module. Consequently, this technique of self-healing is a practical, cost-effective approach for obtaining significant improvement in reliability.

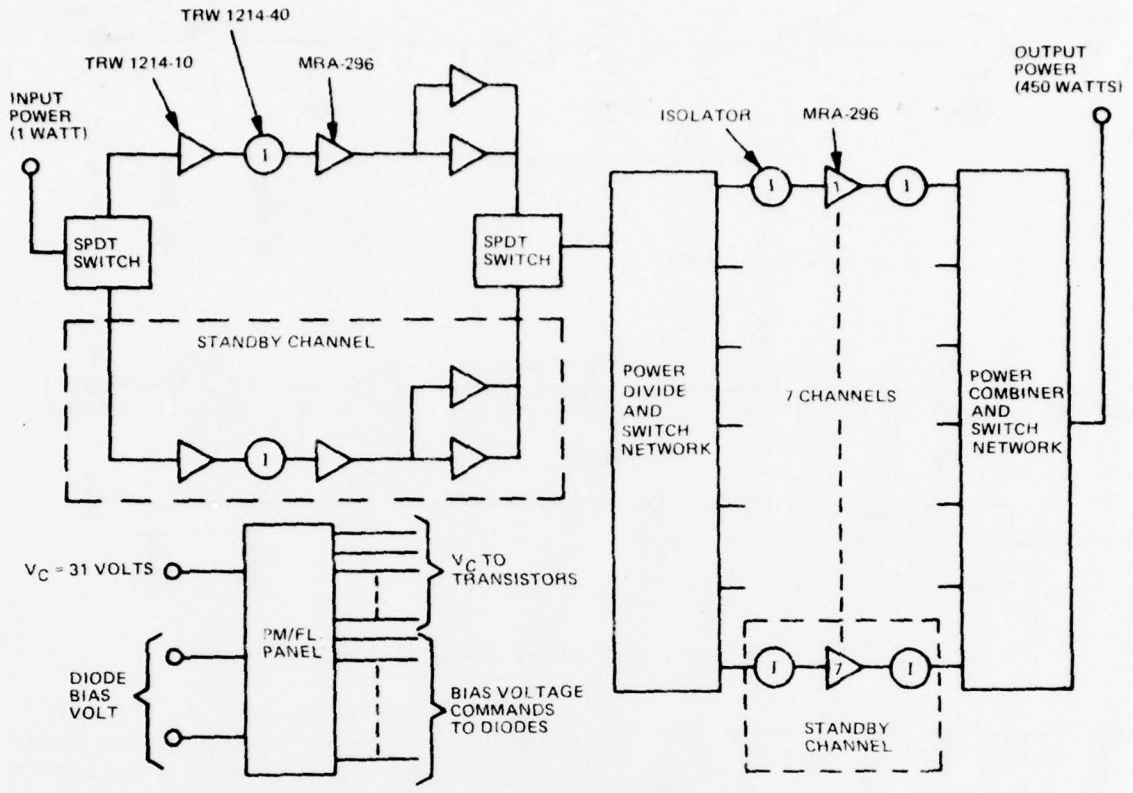

Figure 2-11. Solid State Transmitter, Block Diagram

A performance monitoring and fault locating (PM/FL) panel will be used to provide the sensing, logic, and switching circuits needed to monitor the transistor collector currents and automatically replace a failed amplifier with a standby unit.

A block diagram of the 59 transmit amplifier modules for the low beam signal is presented in figure 2-12. Each of the identical amplifier channels contain three stages of amplification and a duplexer to separate the transmit and receive signals. The duplexer consists of a circulator and a SPDT diode switch arrangement. This configuration efficiently separates the transmit and receive signals, and it also converts the circulator at the output of the module to an isolator during the transmit mode. This protects the output stage from antenna load variations.

The maximum RF transmit output power from any one of the 59 amplifier modules is about 110 watts peak with 1 watt RF input and a collector voltage of 31 volts. This RF output power must be reduced from the maximum value for a range of about 13 dB to provide the desired azimuth illumination taper for sidelobe control. This will be accomplished by reducing the collector supply

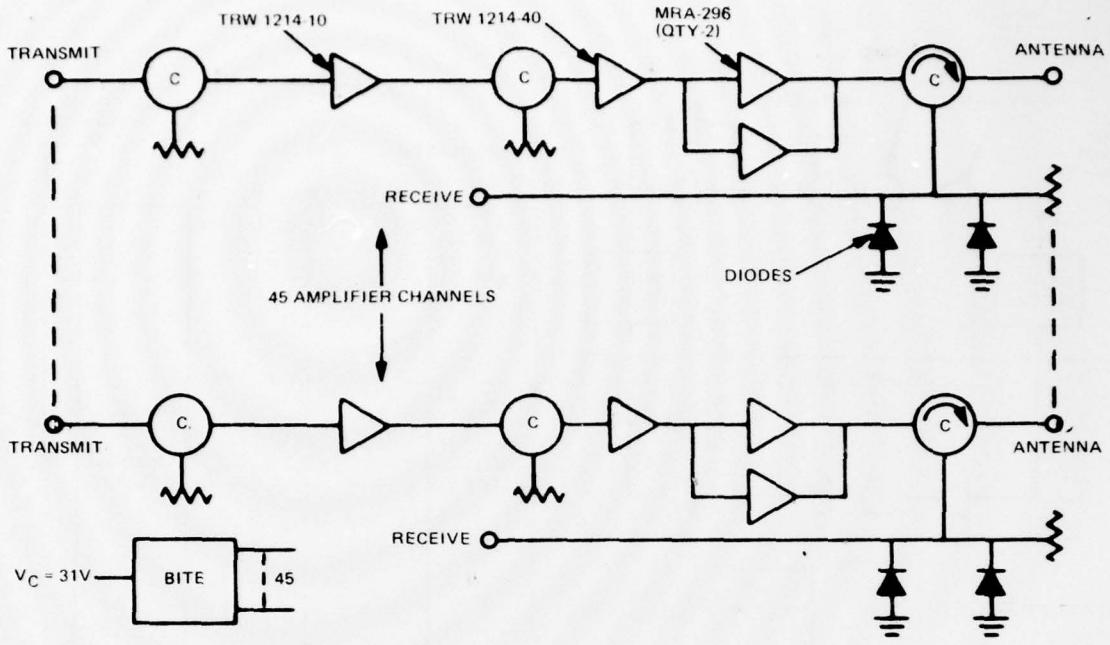

Figure 2-12. Transmit Amplifier Module, Block Diagram

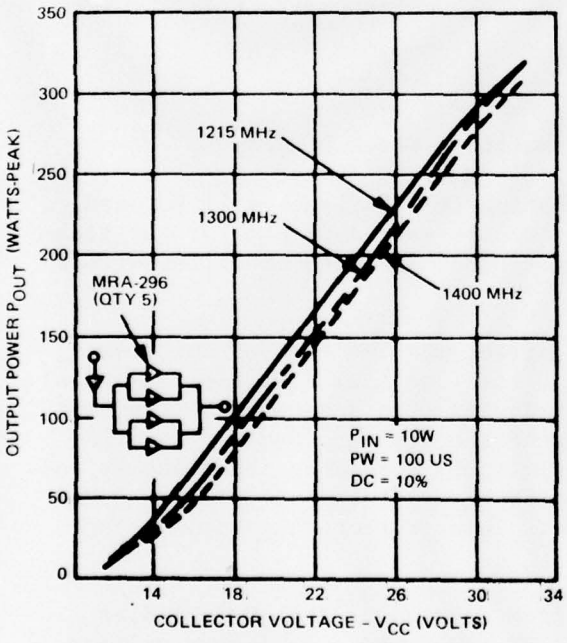

Figure 2-13. Breadboard Module Test Data

voltages where necessary. A typical amplifier response for the output power variation, as a function of a collector voltage, is presented in figure 2-13. The test data are for a two-stage amplifier module, using the MRA-296 transistors, developed for the 2.5-kilowatt L-band amplifier for RADC. As indicated, there is a fairly linear 13 dB reduction of output power as the collector voltage is reduced from 32 volts to 12 volts. Since the proposed transmit amplifier modules contain three stages of amplification, a smaller voltage reduction will be required for the 13 dB output power reduction.

The concept of graceful degradation can be applied for the 59 separate transmit amplifier modules. When one of the transistors fail, the loss of that channel will not seriously affect the array performance. As a result, it is not necessary to use standby amplifiers to achieve the required reliability.

Section 3

DESIGN, FABRICATION, AND TESTING OF A DUAL BEAM COLUMN NETWORK

3.1 TASK SUMMARY

This section describes the progress on the design and fabrication of a stripline dual beam column network. The task is to build a stripline network which will demonstrate both the feasibility of manufacturing a large stripline network and to demonstrate the achievable electrical performance of this network.

3.2 NETWORK DESIGN AND FABRICATION

During the reporting period, the electrical schematic for the network was finalized and the development of all stripline components required to build the network was completed. A layout of the full printed circuit stripline networks was generated using a computer aided design (CAD) machine, and a reduced scale print of the completed layout as plotted by the machine is shown in figure 3-1. The actual full scale printed circuit is 12 feet in length. The information to plot the full network is stored in the CAD memory.

This information is also being translated into Commands to Control a large and extremely accurate Gerber X-Y plotter carrying a light pen. The Gerber plotter and light pen will expose large sheets of photographic film, automatically generating full size photomask negatives of the stripline circuitry. The photomasks are used for contact exposure of photo resist coating in the etching process of the stripline circuits. Prior to this program, negatives for stripline circuits were generally cut by hand on Rubylith with the aid of a coordinograph. The circuits were cut on an enlarged scale and photoreduced for accuracy. However, the unattended radar dual beam column network is so large and complex that it required working out this computer aided technique for automatically plotting the negatives. The technique is being used for a similar large microwave printed circuit which is presently being developed for another program, and which has progressed to the point of completing the Gerber plots for the photomasks, etching the circuits, and satisfactorily testing the etched circuits for electrical performance. The "bugs" have been worked out for this process indicating that the automatic plotting of the photomasks will be successful for the unattended radar column network.

To lay out the network, a final schematic, figure 3-2, was generated. This final schematic differs only in two respects from the original proposed schematic. First, all phase adjustments are accomplished through line lengths rather than Schiffman coupled line flat phase shifters and, second, the line length phase adjustments were added to the outputs to provide a phase gradient across the array to squint the beam 3.65 degrees off the normal.

The decision to use simple line length phase adjustments rather than the more complicated Schiffman flat response phase shifters was made as a result of a computer evaluation of the performance of the network containing only line length phase adjusts. Figure 3-3 is a computer plot of the antenna performance of the column network. The antenna patterns were calculated with

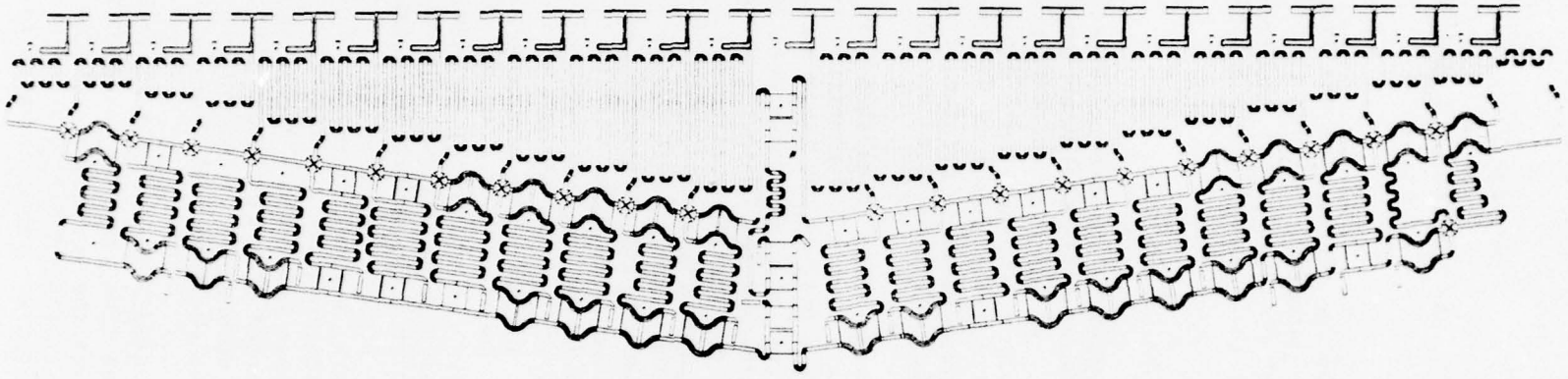

Figure 3-1. Column Network Plotted by CAD Machine

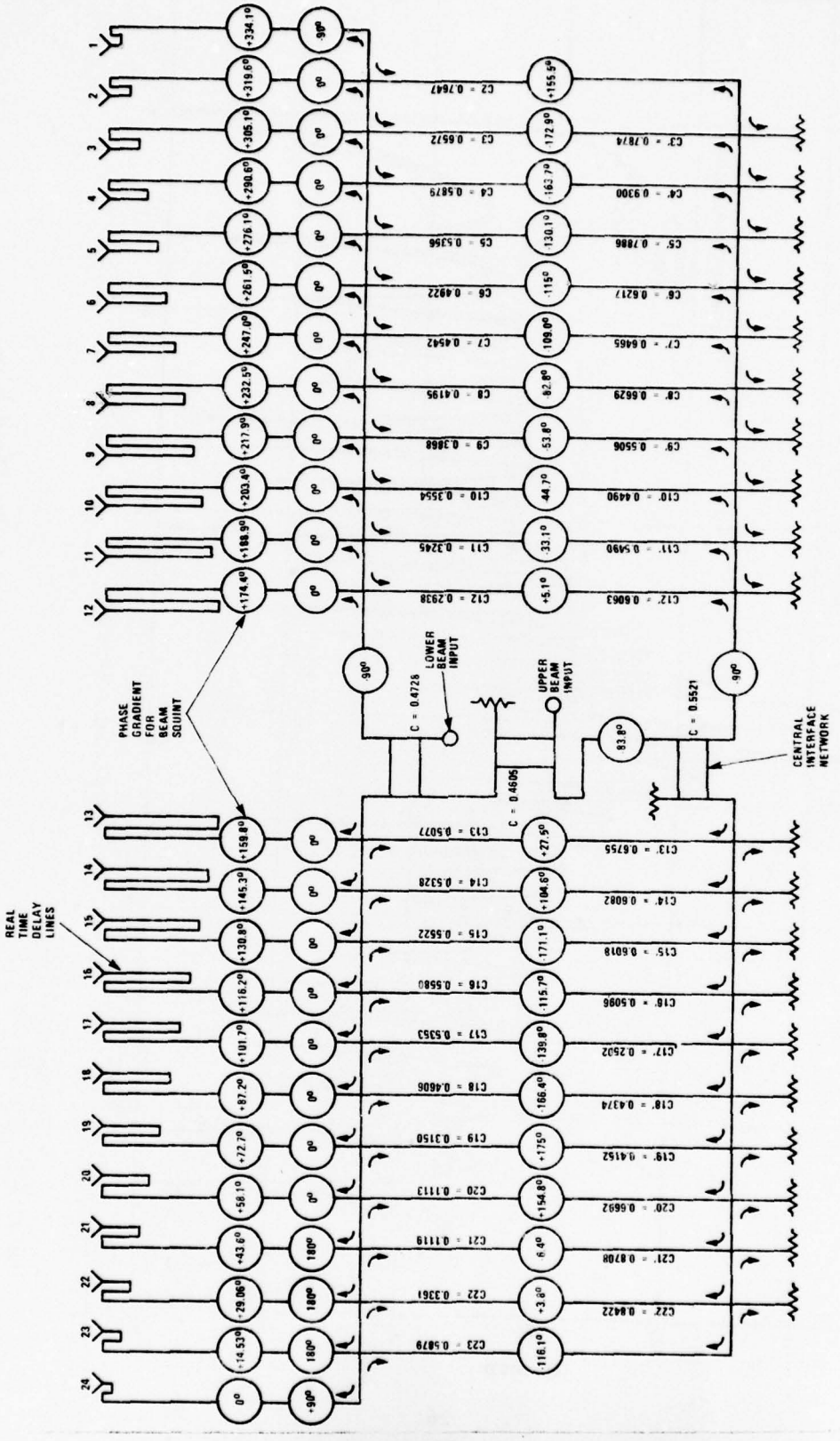

Figure 3-2. Final Schematic

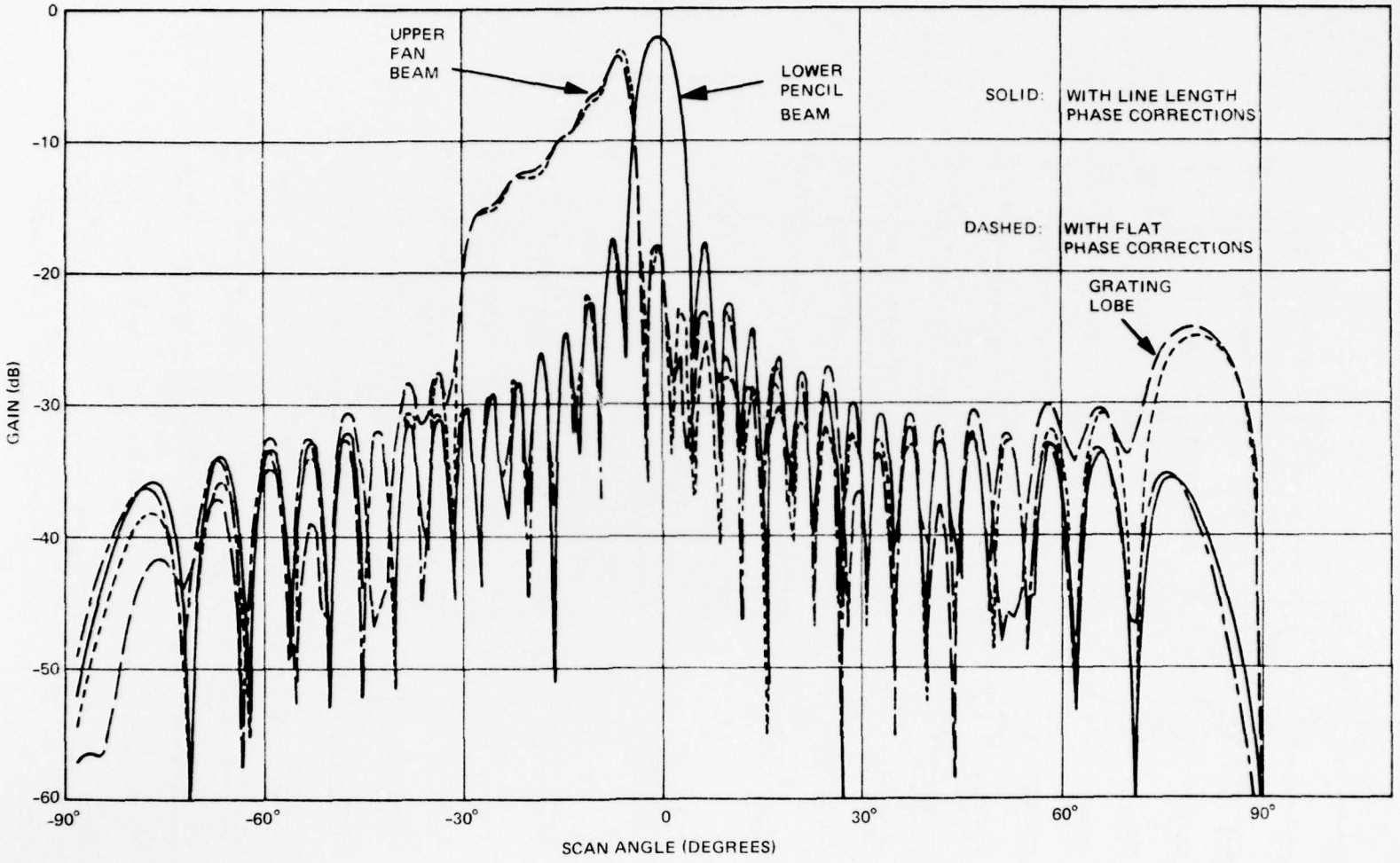

Figure 3-3. Computed Column Network Performance at 1.4 GHz (Band Edge)

both line length phase adjusts and perfect flat phase adjusts. The line length phase adjusts are correct at center band, 1.3 GHz, and deviate to a worst case at band edge, 1.4 GHz, whereas the flat phase adjusts would be correct across the band. Consequently, the patterns were calculated at the band edge for a worst case comparison. As can be seen, there is very little difference between the use of flat phase shifters or the use of line lengths; thus, the line lengths are used in the circuit. This greatly simplifies the design of the circuit since flat Schiffman phase shifters would have been difficult to develop and may have presented some coupling tolerance problems and packaging problems.

The phase tilt is provided to tilt the peak of the lower pencil beam 3.65 degrees below the array normal. The array normal will be tilted 6 degrees above the horizon, so that the lower beam peak will be 2.35 degrees above the horizon to provide the proper coverage. The phase tilt also eliminates the grating lobe on the upper fan beam. This can be seen by comparing figures 3-3 and 3-4. The tilted fan beam is plotted in figure 3.4 with the grating lobe shifted out of real space.

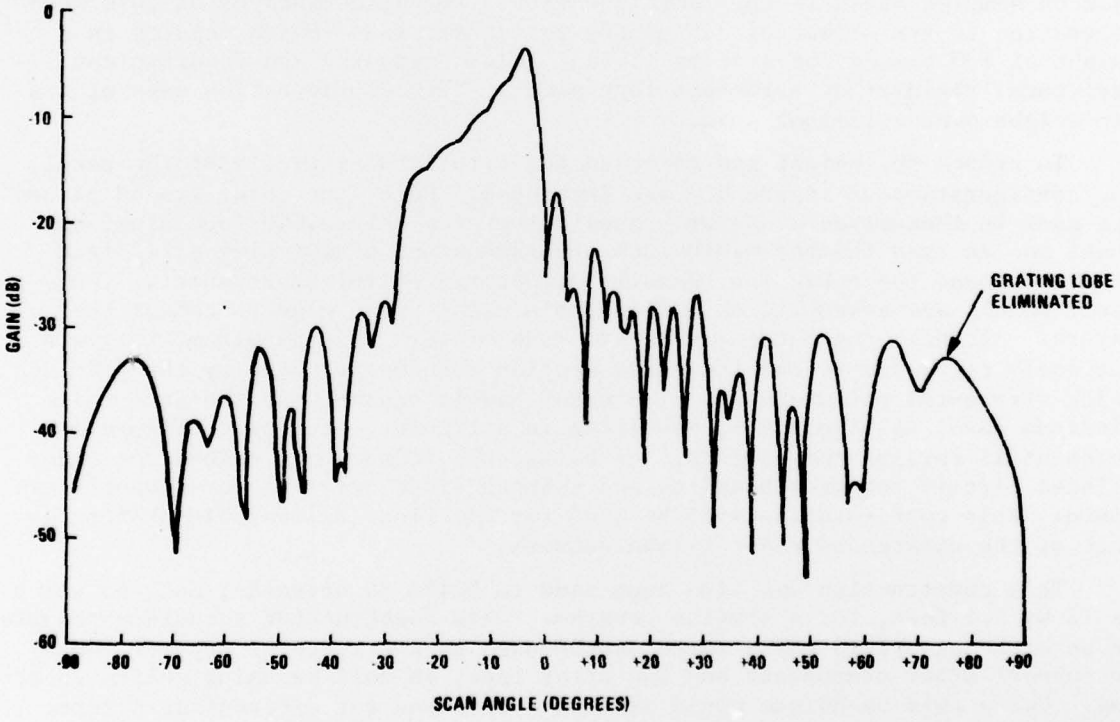

Figure 3-4. Phase Tilted Fan Beam

Section 4

STRIPLINE FABRICATION TECHNIQUES

4.1 TASK SUMMARY

The objectives of this task are to investigate fabrication techniques for the stripline column network with emphasis on electrical performance, ease of manufacturing, cost, structural integrity, and light weight.

4.2 STRIPLINE CONFIGURATIONS

Three basic configurations are being considered and compared for use in the final unattended radar production column networks. The configurations are shown in cross section in figures 4-1, 4-2, and 4-3. The first configuration, figure 4-1, consists of the etched stripline circuit sandwiched between low dielectric constant sheets which are in turn sandwiched between 1/8-inch thick aluminum ground planes. Ground plane spacing is maintained by 1/4-inch thick by 5/8-inch diameter round metal spacers distributed periodically throughout the network. This configuration works well electrically, and it is ideal for breadboarding since the stripline is not permanently captivated between the ground plane, and the network can easily be opened for changes. The dielectric can be spongy foam such as Emerson & Cummings PP or it can be rigid polyurethane since the 1/4-inch thick by 5/8-inch diameter metal spacers provide the ground plane spacing. Loss measurements shown in figure 4-4 have been made on samples built in this configuration. The disadvantages of this configuration is its weight of 3.6 pounds per square foot (which results in a weight of 130 pounds for a 3- by 12-foot column network) and insufficient structural rigidity of a 12-foot long panel. This configuration sags of its own weight over a 12-foot span.

To reduce the weight and increase the structural rigidity of the panel, the configuration of figure 4-2 was developed. Here, the outer ground planes are each in themselves a sandwich consisting of a thin 0.040-inch aluminum sheet and an even thinner 0.010-inch aluminum sheet sandwiching a 1/2-inch thick, 6 pound per cubic foot density structural polyurethane sheet. These outer panels are assembled on a flat table using epoxy glue to cement the layers. Although the outer panels are made of very thin aluminum, they are extremely rigid due to the increased section modulus provided by the 1/2-inch thick structural polyurethane. The outer panels replace the 1/8-inch thick aluminum sheet of figure 4-1, resulting in a lighter, stiffer configuration which still retains the advantage of being able to open and remove the inner printed circuit for breadboarding and changes since only the outer panels are glued. This configuration will be used for the final deliverable prototype unit of the unattended radar column network.

This construction has also been used to build 30 networks, each of which is 12 by 2.5 feet, for a similar program. This construction technique results in an extremely rigid board which can be used as a structural support member to support other components and the array face, as well as being self-supporting. Using this technique could eliminate the need for external structural members. The weight of a 3 x 12-foot panel would be 68 pounds when built in this manner, which is one-half the weight of the original configuration of figure 4-1.

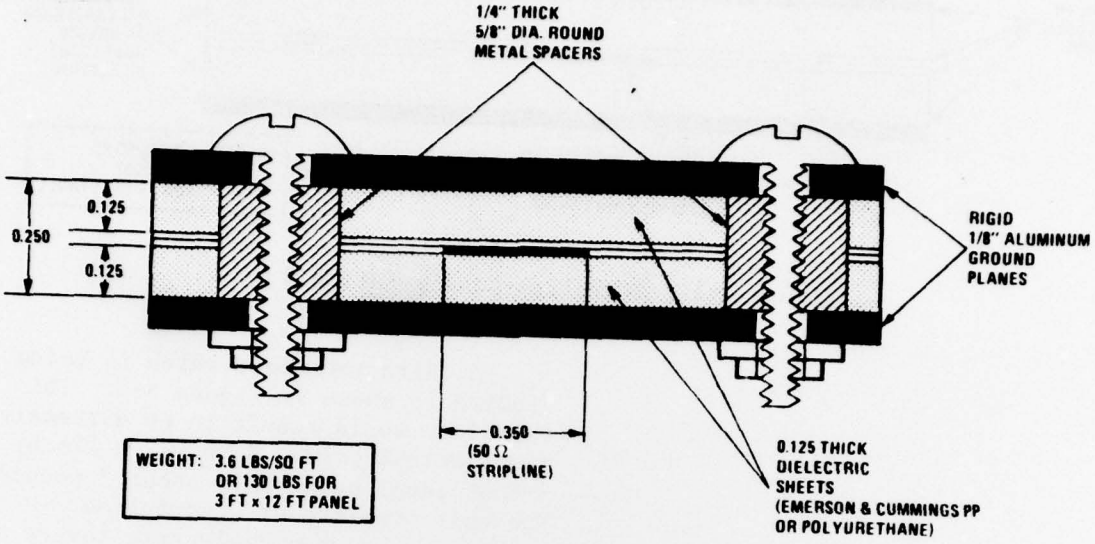

Figure 4-1. Stripline-Configuration 1

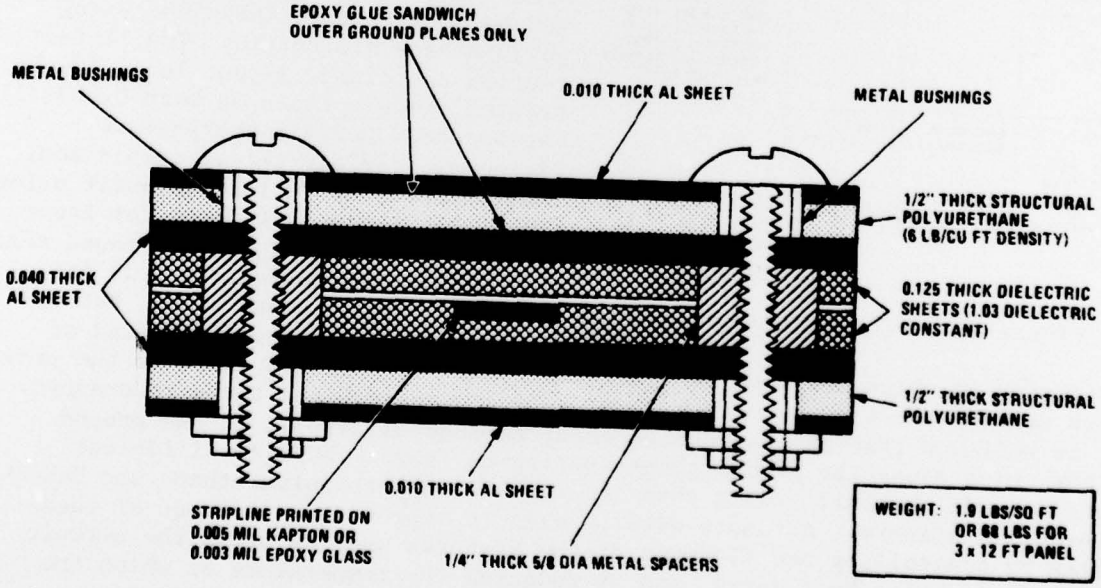

Figure 4-2. Stripline-Configuration 2

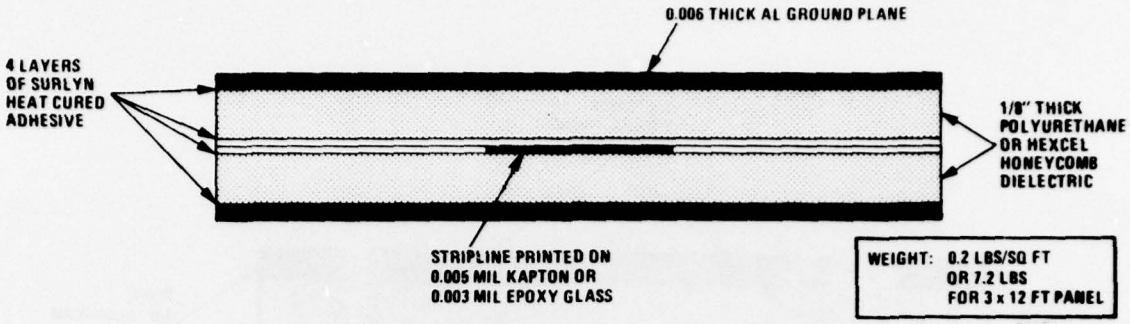

Figure 4-3. Stripline-Configuration 3

MATERIAL	LOSS	λ_g @1.385 GHZ	REMARKS
PP FOAM ($1^{\$}/FT^2$) + KAPTON PC PC ($5^{\$}/FT^2$) 0.003 THICK	0.0045 DB/IN (0.4 DB/7.5 FT)	8.2289" EFF ϵ_r = 1.074	PP SPONGY, CANNOT USE FOR STRUCTURAL SUPPORT. KAPTON EXPENSIVE.
PP FOAM ($1^{\$}/FT^2$) + EPOXY FIBER PC ($2.50/FT^2) 0.005 THICK	0.007 DB/IN (0.63 DB/7.5 FT)	8.1346" EFF ϵ_r = 1.099	EPOXY FIBER PC BOARD CHEAPER THAN KAPTON, BUT MORE LOSSY
TRYMER ($50^{\$}/FT^2$) + KAPTON PC 0.003 THICK			TRYMER RIGID, LOWER LOSS THAN URETHANE. LIKE URETHANE CAN BE STRUCTURAL SUPPORT. SUPERIOR STRUCTURALLY TO PLAIN URETHANE.
TRYMER + EPOXY FIBER PC PC 0.005 THICK	0.0082 DB/IN (0.735 DB/7.5 FT)	8.1425" EFF ϵ_r = 1.096	
HEXCEL POLYURETHANE			

Figure 4-4. Loss Measurements

A third technique which is being studied is shown in figure 4-3. This technique would result in an extremely light weight column Network, a 12- by 3-foot panel being only about 7 pounds. The unit consists of a stripline sandwiched between dielectric layers of polyurethane or HEXCEL which are in turn sandwiched between layers of 0.006-inch thick aluminum sheet. The layers are glued together using 4 layers of Surlyn adhesive sheets which are heat cured in a press in a large oven. A 12-foot experimental section was built with this technique using polyurethane dielectric. The 12-foot section contained 12-foot long, 50-ohm printed circuit lines on both 0.003-mil Kapton and 0.005-mil epoxy-glass dielectric for electrical comparison. The 12-foot board which was built using this technique was measured for insertion loss at L-band. It was found that the loss was approximately 1 dB for either Kapton or epoxy/glass, but exhibited resonances over the band of operation in which the loss increased to 2 dB. Breadboards built in the previous manner (shown in figures 4.1 and 4.2) did not exhibit these resonances. It is believed that the resonances occur because of ripples in the ground plane which cause the ground plane spacing to vary. Additional 12-foot sections will be built using this technique with both polyurethane and HEXCEL dielectric spacers. Attempts will be made to improve the flatness of these units by controlling the flatness of the fixtures used to press the circuit while it is being heat cured, and by reducing the temperature at which the Surlyn glue is cured.

In addition to the lightweight property of the construction technique, the low cost possibility is very attractive. There are fewer parts to fabricate and fewer assembly steps. However, special tools would be required for this assembly procedure for a network of this size. Inquiries have been made of vendors that specialize in procedures similar to those required for the assembly. Information will be available from the vendors during the second half of the program. Also, during the remaining portion of the program, this assembly technique will be evaluated for electrical parameters. The evaluation will determine if ripples in the ground planes can be eliminated or minimized for a network of this length such that insertion loss resonances can be eliminated, as well as the thickness tolerance effect of Hexcel spacing.

Support structure will be required for handling these network boards and to attach dipole ground planes. When the networks are installed into the array, additional structures will be required to take up the effects of wind loads. This additional structure, pro-weighted to each network board, is estimated to be 30 pounds. The resultant 37-pound column network weight is thus 50 percent of foam supported ground plane approach of figure 4-2.

Section 5

DEVELOPMENT OF STRIPLINE COMPONENTS

5.1 TASK SUMMARY

The object of this task was to develop the stripline components required to make the dual beam column network which is described in section 3. The components are 2- and 3-branch directional couplers, crossovers, terminations, and the radiating dipole. The component development is complete, as is the network layout incorporating these components (see figure 3-1).

5.2 BASIC STRIPLINE

The dual channel column network is constructed in a symmetrical stripline configuration which consists of transmission lines etched on 0.003-inch thick Kapton sheets with 0.0014-inch thick copper cladding on one side. The ground plane spacing is 0.250-inch, and is determined by sandwiching the circuit between two 0.125-inch thick polyurethane foam spacer sheets. Thin aluminum sheets form the outer ground planes.

The curves of figure 5-1 were derived from information gathered in past experience on programs which dealt with networks constructed in symmetric stripline supported by materials other than air. These curves depict the phase velocity (V_p), as a function of the strip width to ground plane separation ratio (w/b), for Kapton surrounded by polyurethane foam and for epoxy/fiberglass material surrounded by HEXCEL HRH 10. Figures 5-2 and 5-3 show the characteristic impedance versus w/b for each construction technique.

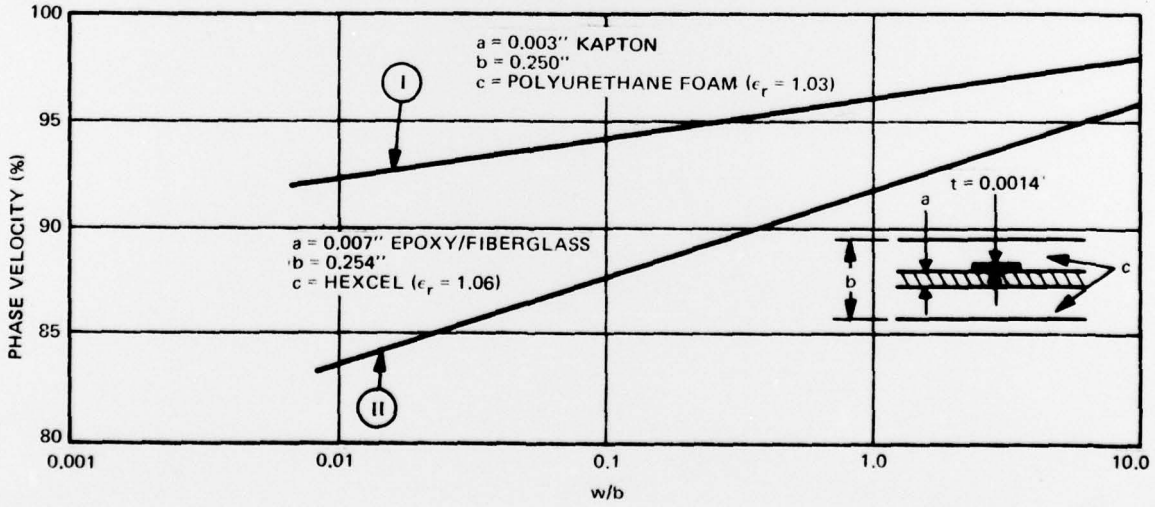

Figure 5-1. Phase Velocity Versus w/b
(Referenced To Air)

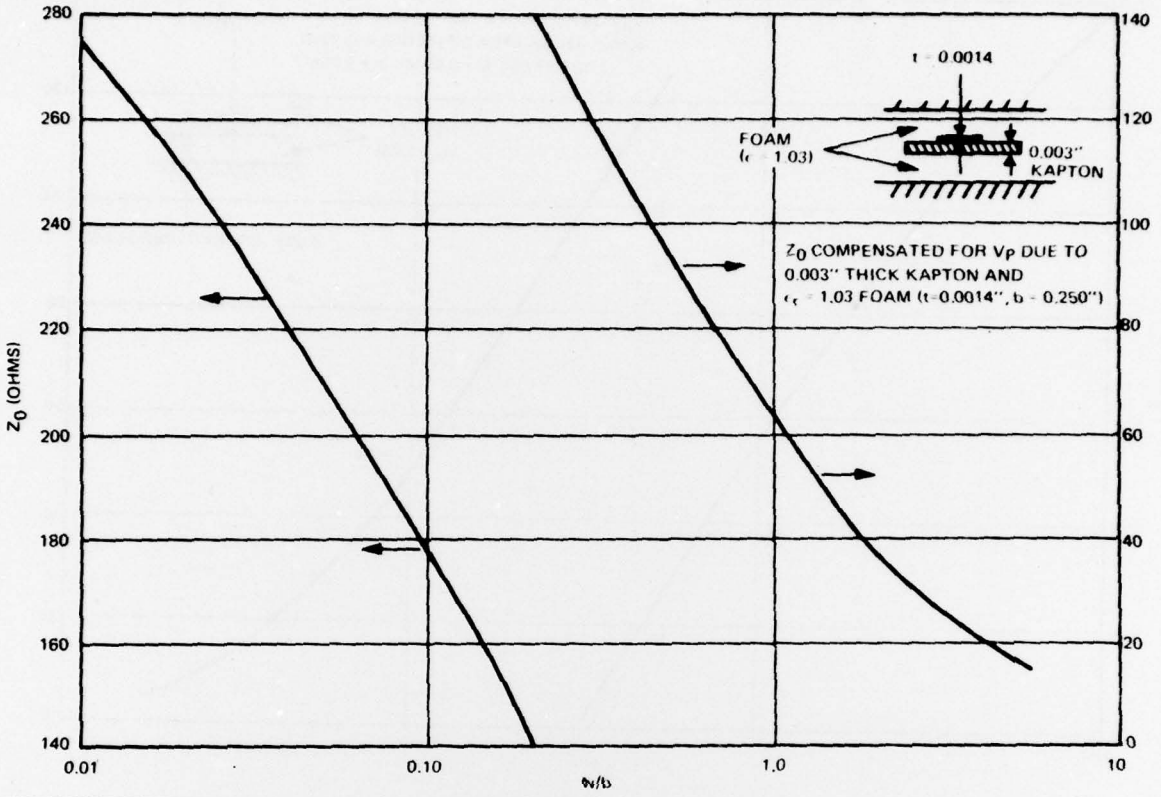

Figure 5-2. Z_0 Versus w/b (Kapton)

5.3 COUPLER DEVELOPMENT

The series feed network requires a total of 43 different coupler designs whose coupling values range from 3.41 dB (C_{max} = 0.6755) to 12.03 dB (C_{min} = 0.2502). The coupler requirements were very influential in determining the feed circuit stripline configuration.

Quarter-wave edge and broadside parallel-coupled structures were considered for this application, but were rejected for the following reasons. The edge-coupled configuration is useful for loose coupling, but is very rarely used for couplers which are tighter than 6 to 8 dB; conversely, the broadside structure is principally used for very tight coupling and is not good for couplers looser than about 6 to 8 dB. Neither coupler is adequate to cover the full range of coupling values required in this network. Additionally, the broadside type requires a three-layer asymmetrical stripline configuration which has inherent registration problems, especially for a circuit of this size and complexity. It would result in a costly package.

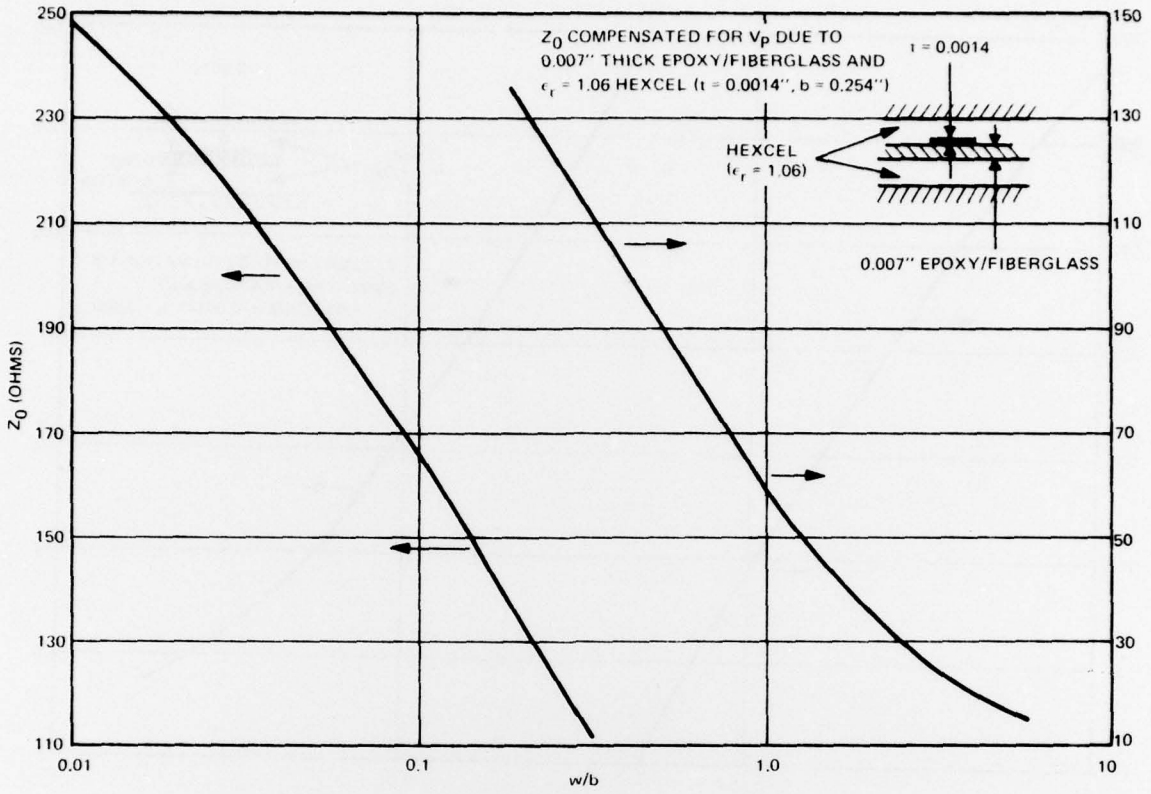

Figure 5-3. Z_o Versus w/b (Epoxy/Fiberglass)

Therefore, branch guide directional couplers were chosen because they can be printed on one side of the stripline sheet and because they are capable of covering the range of coupling values required. Two- and three-branch designs are utilized.

Three-branch couplers are desired throughout the network because of their excellent bandwidth characteristics. However, there is a physical limitation present which governs the use of this type coupler in stripline. It is impractical to print and etch stripline RF lines which are less than 0.010-inch wide and expect a high probability of no defects in the finished product; therefore, it was decided to limit the narrowest line to 0.013-inch. The loosest required three-branch coupler than can be built using this guideline has a coupling value of 6.73 dB. Therefore, couplers ranging from 3.41 dB to 6.73 dB are three-branch, and those from 6.73 db to 12.03 dB are two-branch. The narrowest lines in this loosest two-branch coupler are 0.005-inch. They will be inspected carefully and will be replaced with wire of the proper diameter if found defective. This was done successfully for a

16 dB, two-branch coupler designed for an L-band feed network which Sperry is now building and testing. As seen from the results of a computer analysis, figure 5-4, both type couplers are adequate for this network, displaying very satisfactory VSWR, minimum isolation, and coupling variation characteristics over the band width of interest.

Because it would not be cost-effective to design, build, and test every coupler of the large number required, it was decided to follow the procedure in which five 3-branch couplers, whose coupling values spanned the required range, were selected to be built and tested. Based on those test results, a set of curves was developed which fully describes each physical dimension of any coupler in the range. These curves are shown in figure 5-5. It was determined from computer analysis that optimum results could be achieved by using only two different impedances for the series branches (i.e., 45 ohms for coupling coefficients 0.4 through 0.52, and 40 ohms for C = 0.521 through 0.7). The center shunt arm impedance is dependent on the series arm impedance, thus the reason for two curves to find the width of the center arm. The outer shunt arm impedance depends only on the coupling coefficient and therefore only one curve is necessary. As an example of usage of figure 5-5, if coupling coefficient = 0.50, then A = 0.388, B = 0.020, C = 0.165 inch.

Numerous two-branch couplers were built and tested for a previous L-band column network program at a center frequency slightly higher than that required for this network. Measurements over a bandwidth equal to the unattended radar (15%) bandwidth verified the computer results shown in figure 5-4. It was therefore decided to scale the center frequency of these designs when two-branch couplers were required.

THREE-BRANCH COUPLER

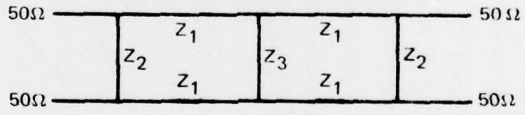

COUPLING	Z_1	Z_2	Z_3	VSWR (BANDEDGES)	MINIMUM ISOLATION	COUPLING VARIATION
3.41dB	40Ω	128.6Ω	47.4Ω	1.048	32.4dB	± 0.058 dB
6.73dB	45Ω	204.9Ω	87.9Ω	1.012	38.5dB	± 0.45dB

TWO-BRANCH COUPLER

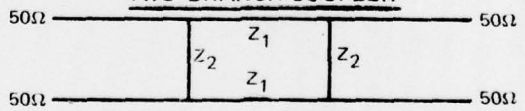

COUPLING	Z_1	Z_2	VSWR (BANDEDGES)	MINIMUM ISOLATION	COUPLING VARIATION
6.73dB	44.38Ω	96.35Ω	1.08	22.2dB	± 0.048dB
12.03dB	48.4Ω	192.7Ω	1.022	28.4dB	± 0.046dB

Figure 5-4. Summary of Results of AMCAP Analysis of Branchline Couplers

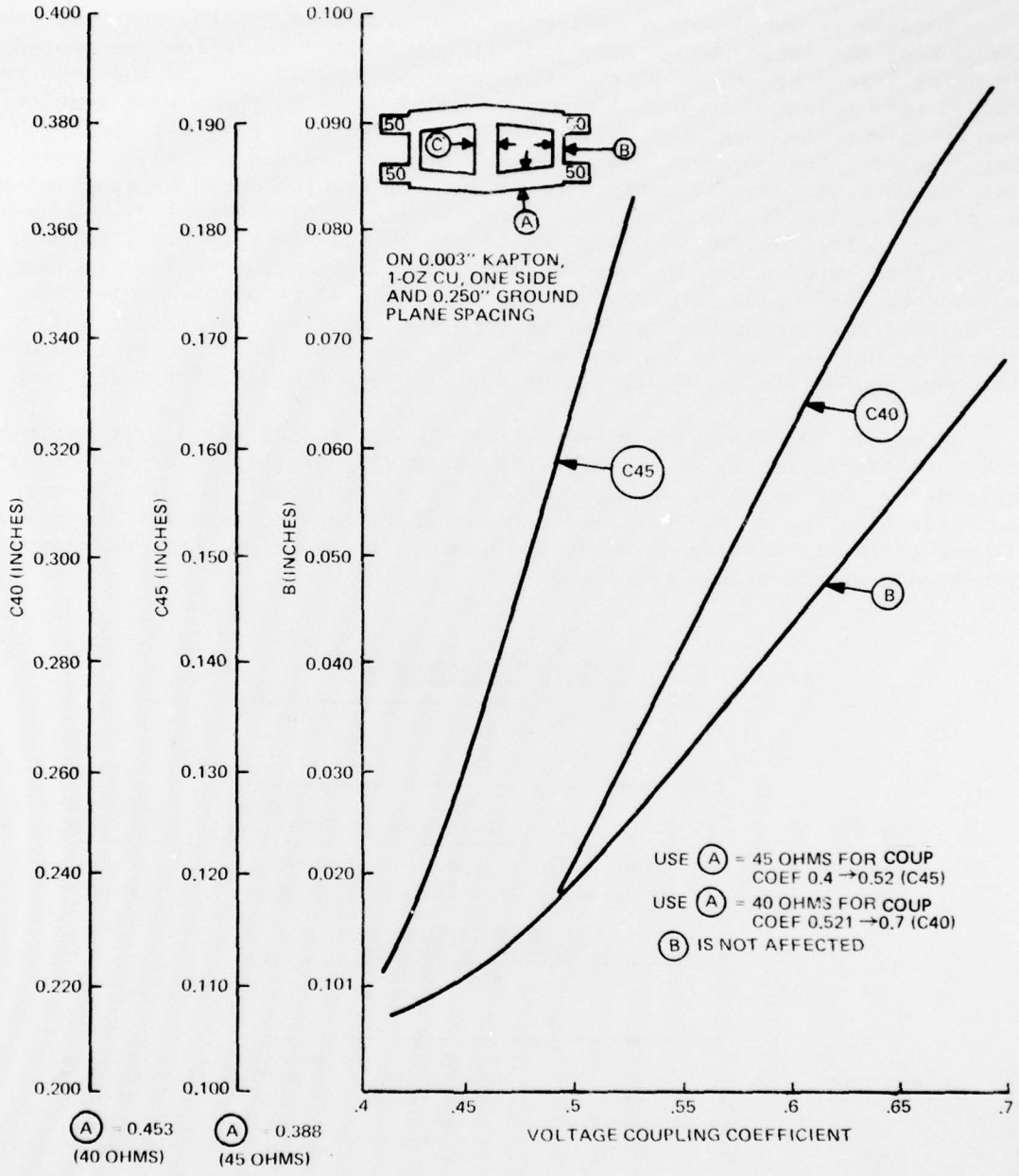

Figure 5-5. Line Widths Versus Coupling Coefficients - Three-Branch Coupler Design

Table 5-1 describes the data taken on the five 3-branch selected couplers. The measured coupling was within 0.1 dB of theoretical, except for the 6.96 dB coupler, which measured within 0.25 dB. Isolation, VSWR, and coupling variation over the bandwidth were all within acceptable limits.

Table 5-1. Data on Five 3-Branch Directional Couplers and Comparison of Measured Results to Theoretical

Theoretical Coupling	Measured Coupling	Maximum VSWR		Minimum Isolation		Coupling Variation	
		Theor.	Meas.*	Theor.	Meas.	Theor.	Meas.
3.41 dB	3.3 dB	1.05	1.04	32.4 dB	24 dB	±.05 dB	±.07 dB
4.61 dB	4.6 dB	1.03	1.11	34.6 dB	28 dB	±.047 dB	±.05 dB
5.9 dB	5.8 dB	1.02	1.09	36.8 dB	28 dB	±.05 dB	±.06 dB
6.96 dB	6.7 dB	1.01	1.12	38.6 dB	28 dB	±.045 dB	±.10 dB
7.6 dB	7.5 dB	1.01	1.12	39.4 dB	26 dB	±.045 dB	±.025 dB

*Maximum VSWR including connectors and terminations.

At the point in time during the development program that these data had been gathered, it was determined from a design layout of the full network that the packaging problems could be significantly lessened if the 3-branch couplers could be made shorter in length. This necessitated development of a folded 3-branch coupler which required bends in series arms of the coupler. The dimensions of the five straight couplers described previously were altered in the following manner: Widths of shunt arms remained the same, whereas the length of the shunt arms were made equal to the algebraic average of the two different original lengths to simplify the design. The length and width of the series arms were modified to reflect the needed higher impedance and the change in phase velocity through the bends. Figure 5-6 shows a comparison of size of the straight and folded three-branch couplers for the 3.3 dB coupling value. Data taken on these folded couplers very nearly matched the data of the straight-arm coupler de-sign. Coupling data were within 0.1 dB of previously measured data. VSWR was as good or better, isolation improved on the average, and coupling variation remained the same (it improved to +0.05 dB for the 6.8 dB coupler). Figure 5-7 is typical

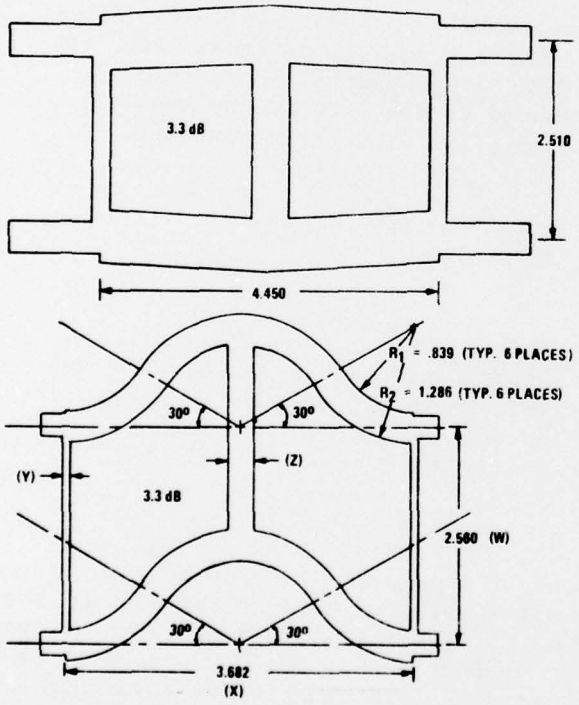

Figure 5-6. Comparison of Size of Straight and Folded Three-Branch Coupler Design

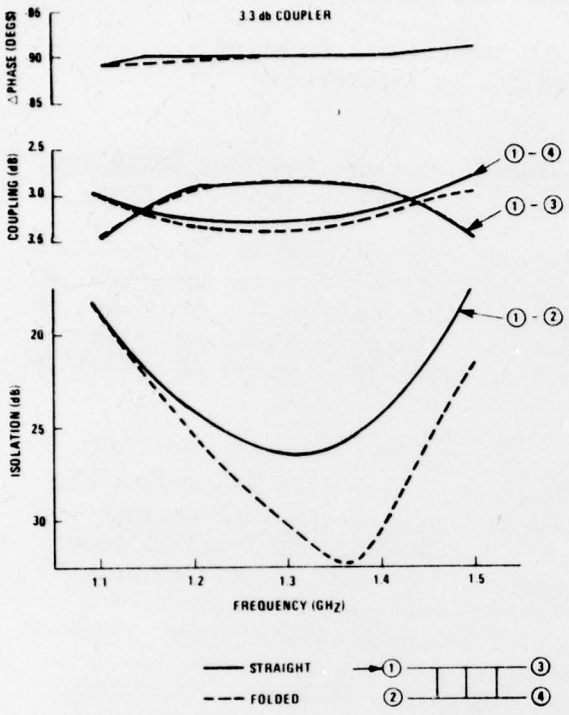

Figure 5-7. Typical Data Results Straight and Folded Three-Branch Coupler

of the data obtained on the three-branch straight and folded couplers.

The three couplers used in the central interlace area of the network are straight three-branch couplers because there is room there for this configuration (see figure 3-1).

Because of the possible weight advantage using HEXCEL in construction of a column netowrk, measurements were taken using HEXCEL HRH 10 as a spacer for a 6.7 dB folded three-branch coupler. The resultant data were no different than that obtained using polyurethane foam spacers and were not dependent on the spacer cell alignment (parallel or perpendicular to the RF line). Therefore, although the first dual column network is being built using Emerson and Cummings PP dielectric, it will be possible to substitute any other dielectric such as HEXCEL or TRYMER in the final configuration so long as it has a low dielectric constant (1.03). The network itself is designed with "real time" line lengths and therefore should not be affected by small changes in dielectric constant.

5.4 TERMINATIONS

Terminations for all couplers were designed, built, and tested. They consist of a 51-ohm, 1/4-watt, carbon resistor, soldered in series with the 50-ohm RF line, terminated by an open-circuit length of 50-ohm line. This open-circuit length of line ($< \lambda/4$) matches out the inductive reactance of the resistor. VSWR is less than 1.15:1 over the bandwidth.

5.5 CROSSOVERS

The crossovers included in the layout of figure 3-1 consist of printed arrows with crossed 0.020-inch diameter wires soldered between the tips of the arrows. This design is inexpensive and lends itself well to any of the stripline construction techniques as described in Section 4. The 0.020-inch wires are inductive and are matched by the arrows which are capacitive, forming a low pass filter. This design has a VSWR which rises to a high of 1.2 at the upper end of the operating band (1.4 GHz). In addition, its isolation is

limited to 25 to 30 dB. Studies have shown that the isolation is tolerable in the network design, while the VSWR may be tolerable since the crossovers are spaced approximately 3/4 of a wavelength apart and are also padded by the coupler between each crossover.

The breadboard will be built using the printed arrow crossover, but should the electrical performance be inadequate, another crossover design will be substituted. This is a crossed coaxial line design which has an excellent match (< 1.05) and very high isolation (> 50 dB). However, the coax design is more expensive and will only be used if the measured breadboard network performance is inadequate.

5.6 PRINTED CIRCUIT DIPOLE

The dipole design used in the layout of figure 3-1 is a design developed for the Sperry AN/TPS-59 and ALR antenna. The measured VSWR of a single dipole over a ground plane was less than 1.1 at 1.3 GHz rising to 1.45 at the band edges. It is felt that this dipole will be adequate to demonstrate the performance of a single line source, and is included in the layout. Attempting to improve the VSWR at this time would not be advantageous since the dipole match is highly dependent on the spacing of the elements in an array environment. Since only a line source will be built at this time, fine tuning of the dipole VSWR wil not be possible.

MISSION
of
Rome Air Development Center

RADC plans and executes research, development, test and selected acquisition programs in support of Command, Control Communications and Intelligence (C^3I) activities. Technical and engineering support within areas of technical competence is provided to ESD Program Offices (POs) and other ESD elements. The principal technical mission areas are communications, electromagnetic guidance and control, surveillance of ground and aerospace objects, intelligence data collection and handling, information system technology, ionospheric propagation, solid state sciences, microwave physics and electronic reliability, maintainability and compatibility.

Printed by
United States Air Force
Hanscom AFB, Mass. 01731